OH and HO2 chemistry during NAMBLEX: Roles of oxygenates, halogen oxides and neterogeneous uptake

Sommariva, R; Pilling, M; Bloss, William; Heard, D; Carslaw, N; Lewis, A; McFiggan, G; Plane, J; Saiz-Lopez, A; Monks, P

Atmos. Chem. Phys., 6, 1135–1153, 2006
www.atmos-chem-phys.net/6/1135/2006/

Atmospheric Chemistry and Physics

OH and HO_2 chemistry during NAMBLEX: roles of oxygenates, halogen oxides and heterogeneous uptake

R. Sommariva[1,*], W. J. Bloss[1], N. Brough[3], N. Carslaw[4], M. Flynn[6], A.-L. Haggerstone[2], D. E. Heard[1], J. R. Hopkins[2], J. D. Lee[1,], A. C. Lewis[2], G. McFiggans[6], P. S. Monks[5], S. A. Penkett[3], M. J. Pilling[1], J. M. C. Plane[3], K. A. Read[1], A. Saiz-Lopez[3], A. R. Rickard[5,***], and P. I. Williams[6]**

[1]School of Chemistry, University of Leeds, Leeds, UK
[2]Department of Chemistry, University of York, York, UK
[3]School of Environmental Sciences, University of East Anglia, Norwich, UK
[4]Environment Department, University of York, York, UK
[5]Department of Chemistry, University of Leicester, Leicester, UK
[6]School of Earth, Atmospheric & Environmental Sciences, University of Manchester, Manchester, UK
*now at: Earth System Research Laboratory, National Oceanic and Atmospheric Administration, Boulder, CO, USA
**now at: Department of Chemistry, University of York, York, UK
***now at: School of Chemistry, University of Leeds, Leeds, UK

Received: 26 August 2005 – Published in Atmos. Chem. Phys. Discuss.: 1 November 2005
Revised: 3 February 2006 – Accepted: 9 February 2006 – Published: 5 April 2006

Abstract. Several zero-dimensional box-models with different levels of chemical complexity, based on the Master Chemical Mechanism (MCM), have been used to study the chemistry of OH and HO_2 in a coastal environment in the Northern Hemisphere. The models were constrained to and compared with measurements made during the NAMBLEX campaign (Mace Head, Ireland) in summer 2002.

The base models, which were constrained to measured CO, CH_4 and NMHCs, were able to reproduce [OH] within 25%, but overestimated [HO_2] by about a factor of 2. Agreement was improved when the models were constrained to oxygenated compounds (acetaldehyde, methanol and acetone), highlighting their importance for the radical budget. When the models were constrained to measured halogen monoxides (IO, BrO) and used a more detailed, measurements-based, treatment to describe the heterogeneous uptake, modelled [OH] increased by up to 15% and [HO_2] decreased by up to 30%. The actual impact of halogen monoxides on the modelled concentrations of HO_x was dependant on the uptake coefficients used for HOI, HOBr and HO_2. Better agreement, within the combined uncertainties of the measurements and of the model, was achieved when using high uptake coefficients for HO_2 and HOI (γ_{HO_2}=1, γ_{HOI}=0.6).

A rate of production and destruction analysis of the models allowed a detailed study of OH and HO_2 chemistry under the conditions encountered during NAMBLEX, showing the importance of oxygenates and of XO (where X=I, Br) as co-reactants for OH and HO_2 and of HOX photolysis as a source for OH.

Correspondence to: M. J. Pilling
(m.j.pilling@leeds.ac.uk)

1 Introduction

The chemistry of the troposphere during the day is controlled by the concentration of the OH and HO_2 radicals. These two species are the key components of a radical cycle that oxidizes the trace gases in the lower atmosphere. The ability to simulate HO_x is therefore a good test of our understanding of the chemical processes of the troposphere.

The main source of OH in the troposphere is the reaction of water vapour with $O(^1D)$, from ozone photolysis (Reactions R1–R2)

$$O_3 + h\nu \rightarrow O_2 + O(^1D) \quad \text{(R1)}$$

$$O(^1D) + H_2O \rightarrow 2\ OH \quad \text{(R2)}$$

OH reacts with CO to give HO_2 and with CH_4 and a range of Non Methane Hydrocarbons (NMHCs) to give a large number of organic peroxy radicals (RO_2), the most important of which is CH_3O_2.

In the presence of NO_x the peroxy radicals react with NO forming HO_2 through the reaction of the alkoxy radical with O_2. This is not the only fate of the alkoxy radicals, which

Published by Copernicus GmbH on behalf of the European Geosciences Union.

can also decompose or isomerize to form other alkyl radicals and/or carbonyl compounds. The formation of alkylnitrates (RCH_2ONO_2) and peroxyalkylnitrates ($RCH_2O_2NO_2$) can also be important, in particular for long chain alkylperoxy radicals (>C5) and for peroxyacetyl radicals, respectively (Atkinson and Arey, 2003). At low NO_x the peroxy radicals primarily react through self and cross peroxy-peroxy reactions to form peroxides (e.g., H_2O_2 and CH_3OOH).

The formation of HO_2 in these processes leads to the reformation of OH through the reactions with O_3 and, in high NO_x conditions, NO, thus closing the radical cycle. The peroxides act as sources and sinks of OH through their photolysis or reaction with OH.

Carbonyls are important intermediates. They typically form from the decomposition of alkoxy radicals (e.g., HCHO from CH_3O and CH_3CHO from C_2H_5O) and they act both as sources, via photolysis, and as sinks, via reaction with OH, of radicals (Reactions R3–R4). In this way they have a large influence on the radical budget.

$$CH_3CHO + h\nu\ (+2\ O_2) \rightarrow CH_3O_2 + HO_2 + CO \qquad (R3)$$

$$CH_3CHO + OH\ (+O_2) \rightarrow CH_3CO_3 + H_2O \qquad (R4)$$

Several modelling studies have been performed for the marine boundary layer (MBL) chemistry. Typically OH is overestimated by a factor of 1.1 (Sommariva et al., 2004 at Cape Grim, Tasmania, SOAPEX-2 campaign, 1999) up to a factor of 2.4 (Carslaw et al., 2002, at Mace Head, Ireland, EASE97 campaign, 1997). During two aircraft campaigns in the Pacific Ocean, OH was underestimated by up to 30% (Olson et al., 2004). HO_2 is generally overestimated by a factor of 1.2 (Kanaya et al., 2001, at Okinawa, Japan, Orion99 campaign, 1999) up to a factor of 3.6 (Carslaw et al., 2002 at Mace Head, Ireland, EASE97 campaign, 1997). The model-measurements comparison for HO_2 was much better during the PEM Tropics B aircraft campaign, when the average model/measurement ratio was about 1.03 (Tan et al., 2001). A more complete review of the model/measurement comparisons of OH and HO_2 in the MBL and in other environments can be found in Heard and Pilling (2003).

This paper reports a modelling study of OH and HO_2 in the clean marine boundary layer during the NAMBLEX (North-Atlantic Marine Boundary Layer Experiment) campaign using a set of observationally constrained box-models based upon the Master Chemical Mechanism (Jenkin et al., 1997, 2003; Saunders et al., 2003). Sections 2, 3 and 4 of this paper describe the NAMBLEX site, the procedure used to estimate photolysis rates and the models that were used. Section 5 describes the results of the models and the comparison with the measurements, while Sect. 6 discusses possible ways to reduce the discrepancy between the model and the measurements. The results of the improved models are discussed in Sect. 7 and analyzed in Sect. 8. The conclusions are drawn in Sect. 9.

2 The NAMBLEX campaign

The NAMBLEX campaign was conducted at Mace Head, Ireland, between 23 July and 4 September 2002. The aim of the campaign, which involved ten British universities (Aberystwyth, Bristol, Birmingham, Cambridge, East Anglia, Edinburgh, Leeds, Leicester, UMIST, York) and the National University of Ireland, Galway, was to study the chemistry of the marine boundary layer under clean conditions in the Northern Hemisphere. A full overview of the campaign can be found in Heard et al. (2005). The Mace Head Atmospheric Research Station is located at 53°20′ N, 9°54′ W on the western coast of Ireland, about 90 km from Galway. The station is part of the Global Atmospheric Watch program of the World Meteorological Organization (http://www.wmo.ch/web/arep/gaw/gaw_home.html) and of the AGAGE program (http://agage.eas.gatech.edu/) and consists of two laboratories and two towers (21 m and 10 m) situated about 100 m from the shore. A third laboratory is situated about 300 m from the shore and 25 m above sea level. Most of the instruments during NAMBLEX were located inside or around the shore laboratories within a radius of about 10–20 m. The measurements and the techniques used during NAMBLEX are listed in Heard et al. (2005). Further information about the station and the facilities can be found in Jennings et al. (2003) and at http://macehead.physics.nuigalway.ie/.

Meteorological conditions during NAMBLEX are discussed in detail in Norton et al. (2006). Apart from a short period at the beginning of August when air masses arrived at Mace Head from the north-east, bringing pollution from Scandinavia and northern Britain, most of the time the air sampled was of oceanic origin. The five-day back trajectories (Fig. 1) show that air masses travelled across the Atlantic from North America (west trajectories), Greenland (north-west trajectories) and from the tropics (south-west trajectories).

Table 1 shows the 24 h average concentrations and values of some significant variables measured during the campaign during some selected days. The modelling work was concentrated on four clean days (9, 10, 31 August and 1 September) and on the week 15–21 August, when all the measurements used by the models were available (Sect. 4). The clean days were characterized by westerly and north-westerly trajectories and low NO_x concentrations (<30 ppt of NO and 60–80 ppt of NO_2). Acetylene was around 50 ppt on 9–10 August and around 100 ppt on 31 August and 1 September. The week from 15 to 21 August was characterized by unusual anticyclonic conditions which caused the air masses to stagnate off the Irish coast for several days. During this period, [NO] was on average quite low (10–20 ppt), with the exception of two days (16 and 21 August), when it was on average between 70 and 100 ppt. The concentration of NO_2 was high on 16, 20 and 21 August (100–240 ppt), but rather low on 15, 17, 18 and 19 August (20–50 ppt). The low [NO]/[NO_2] ratio on 16, 20 and 21 August was indicative of the absence of

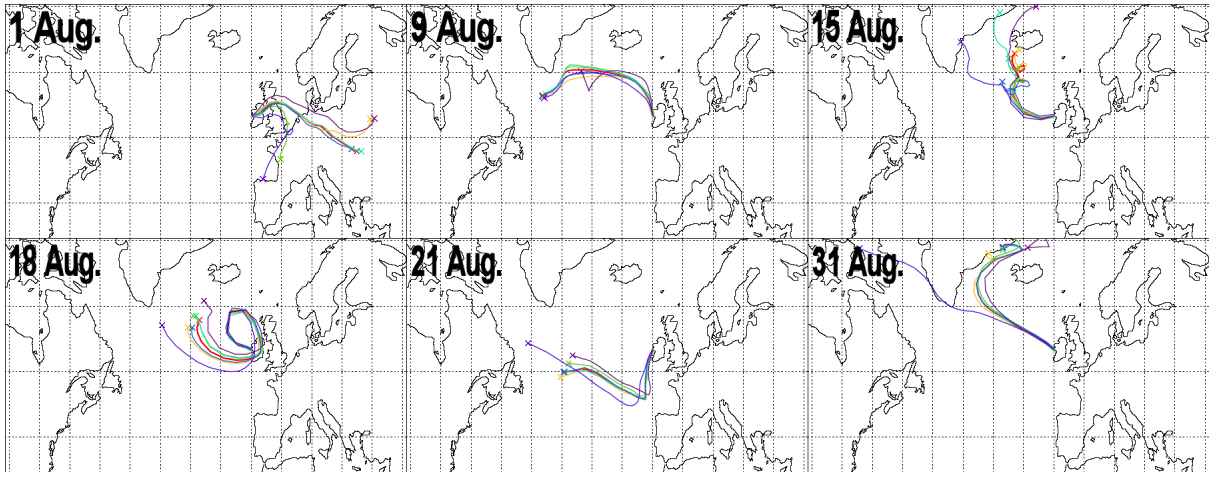

Fig. 1. Clusters of five-day back trajectories for some selected days during NAMBLEX. Different colors indicate trajectories released from different points around Mace Head (Heard et al., 2005; Methven et al., 2001).

Table 1. Average (24 h) measurements on some selected days during NAMBLEX.

Measurements	1 Aug	9 Aug	15 Aug	18 Aug	21 Aug	31 Aug
O_3/ppb	26	31	31	32	26	32
NO/ppt	52	13	7	14	70	15
NO_2/ppt	334	77	28	51	215	54
CH_4/ppb	1956	1813	1798	–	1837	1815
CO/ppb	142	79	79	–	80	104
H_2/ppb	550	–	495	–	511	493
HCHO (UEA)/ppt	545	376	78	257	314 [a]	–
HCHO (Leeds)/ppt	1449	801	664	754	827 [b]	–
Isoprene/ppt	15	9	1	20	32	1
DMS/ppt	131	73	183	115	54	87
Acetylene/ppt	195	49	41	65	55	104
Acetaldehyde/ppt	732	436	674	676	389	236
Temperature/°C	16.8	14.4	15.2	15.5	15.8	14.8

[a] partial data (13:30–14:50 and 15:20–20:15).
[b] partial data (00:00–09:45).

fresh emissions of nitrogen oxides. The toluene/benzene ratio was always <1 during the week 15–21 August and often <0.5, which indicated a long chemical processing of the air masses under anticyclonic conditions (the toluene:benzene ratio at source was assumed 4.4, Lewis et al., 2005). Average acetylene concentrations were between 40 and 70 ppt throughout the week. In practice, 15, 17, 18 and 19 August can be considered as clean days, on the basis of the low concentrations of NO_x and acetylene.

3 Estimation of photolysis rates

Photolysis rates, particularly those of O_3 (Reaction R1) and NO_2, are key constraints to the models. During the NAMBLEX campaign, photolysis rates were measured using three filter radiometers and a spectral radiometer (Edwards and Monks, 2003). The spectral radiometer allowed the measurement of other important photolysis rates, such as j(HCHO), j(CH_3CHO), j(CH_3COCH_3), j(HONO, j(HOI) and j(HOBr).

However, there were days throughout the campaign (1, 2, 15, 17 August and 1 September), when these data were not available, owing to power failures or computer crashes.

Table 2. Correlation equations between photolysis rates on 30 July and 31 August ($HCHO_{(r)}$ is the radical channel of HCHO photolysis; $HCHO_{(nr)}$ is the non-radical channel of HCHO photolysis).

$j(CH_3CHO)$ vs. $j(O^1D)$		R^2
30 July	$1.39\times10^{8}x^3-5.86\times10^{3}x^2+2.27\times10^{-1}x-1.86\times10^{-9}$	0.999
31 August	$1.06\times10^{8}x^3-4.41\times10^{3}x^2+2.08\times10^{-1}x+8.78\times10^{-9}$	0.9994
$j(CH_3COCH_3)$ vs. $j(O^1D)$		R^2
30 July	$1.17\times10^{7}x^3-4.65\times10^{2}x^2+2.69\times10^{-2}x-5.36\times10^{-10}$	0.9995
31 August	$7.23\times10^{6}x^3-2.85\times10^{2}x^2+2.49\times10^{-2}x-5.54\times10^{-10}$	0.9996
$j(HCHO_{(r)})$ vs. $j(O^1D)$		R^2
30 July	$-6.65\times10^{13}x^4+5.62\times10^{9}x^3-1.50\times10^{5}x^2+2.40x+8.07\times10^{-8}$	0.9933
31 August	$1.55\times10^{5}x^5-1.02\times10^{15}x^4+2.05\times10^{10}x^3-2.86\times10^{5}x^2+2.47x+1.67\times10^{-7}$	0.996
$j(HCHO_{(nr)})$ vs. $j(O^1D)$		R^2
30 July	$-1.19\times10^{14}x^4+1.20\times10^{10}x^3-3.49\times10^{5}x^2+4.89x+4.92\times10^{-7}$	0.9661
31 August	$5.85\times10^{19}x^5-3.60\times10^{15}x^4+8.21\times10^{10}x^3-8.59\times10^{5}x^2+5.50x+4.59\times10^{-7}$	0.989
$j(HONO)$ vs. $j(NO_2)$		R^2
30 July	$-3.56\times10^{-1}x^2+2.00\times10^{-1}x-3.38\times10^{-6}$	0.9991
31 August	$8.21\times10^{-1}x^2+1.99\times10^{-1}x-4.03\times10^{-7}$	0.9995
$j(HOI)$ vs. $j(NO_2)$		R^2
31 August	$892.43x^3-6.7234x^2+1.0761x-6\times10^{-6}$	0.9998

$j(O^1D)$ and $j(NO_2)$ data could be replaced by the filter radiometer measurements, but it was necessary to find a way to estimate the missing data. One methodology that has been proposed uses correlations between $j(O^1D)$ or $j(NO_2)$ and the other photolysis rates (Kraus and Hofzumahaus, 1998). This approach is based on the similar wavelength dependencies of the photolysis rates of species with similar absorption spectra.

Acetone and acetaldehyde photolyze in the same range of wavelength ($290<\lambda<330$ nm) which is very similar to $j(O^1D)$. j(HONO) and j(HOI) photolysis rates are approximately in the same wavelength interval as $j(NO_2)$. Using this approach, a procedure in three steps was developed to estimate the photolysis rates for the days with gaps in the spectral radiometer measurements:

1. Spectral radiometer data from the nearest day with complete measurements were used to find a correlation between $j(O^1D)$ or $j(NO_2)$ and the photolysis rates of interest (j(HONO), j(HCHO), $j(CH_3CHO)$, $j(CH_3COCH_3)$ and j(HOI)).
2. The correlations were used with $j(O^1D)$ and $j(NO_2)$ data from the filter radiometer to estimate j(HONO), j(HCHO), $j(CH_3CHO)$, $j(CH_3COCH_3)$ and j(HOI) during the gaps.
3. The difference between the estimated values and the spectral radiometer data before and after the gaps was calculated to estimate the error in using the correlation.

To achieve a better correlation between the parameters and to take into account the differences in the absorption cross sections of the molecules, polynomial correlations were used. The correlation was usually very good with $R^2\geq0.9$ for all species (Table 2). The data for HCHO showed a larger scatter than those for the other compounds. While HCHO photolyzes roughly in the same region of O^1D production from O_3 in the lower troposphere ($300<\lambda<340$ nm), the HCHO spectrum is highly structured, unlike that of O_3. The correlation parameters were slightly different from day to day, reflecting the differences in the position of the sun and the variability of light intensity (Table 2).

Using these correlations and the filter radiometer data it was possible to estimate the photolysis rates for j(HONO), j(HCHO), $j(CH_3CHO)$, $j(CH_3COCH_3)$ and j(HOI) in the periods when the measurements were not available.

The difference between the estimated and the measured photolysis rates before and after the gaps was in most cases less than 30% and occasionally within 50%, which is comparable to the instrumental uncertainties. The difference was much higher (up to 200%) at high solar zenith angles (SZA),

due to the different responses of the filter and spectral radiometers, which becomes more appreciable at SZA $>70°$ (Bohn et al., 2004). Owing to the fixed band width of the filter radiometers, these types of instruments do not perform well at high solar zenith angles, because of the increased path length of radiation through the atmosphere, which increases the relative proportion of the diffuse (scattered) component of light. Therefore caution should be applied when using this type of correlations to estimate the photolysis rates. The time of the day when the gaps in the measurements occur could significantly affect the estimate. It may, however, not affect the modelling results if the species which is photolyzed has little overall effect on the radical budget.

The main advantage of using this procedure to estimate photolysis rates, instead of calculating them with a model, is that the short term variability due to clouds can be taken into account. However, clouds can both attenuate (homogeneous field) and enhance (broken field) the actinic flux. This effect has recently been shown to be non-linear with respect to spectral function and hence photolysis rates will also not scale linearly under cloudy conditions (Monks et al., 2004). These cloud effects are also increased at higher SZA, making the estimation even less reliable at those SZA.

4 The models

The construction of the models for NAMBLEX followed the same guidelines explained in Carslaw et al. (1999); Sommariva et al. (2004). Version 3.1 of the Master Chemical Mechanism (MCM, http://mcm.leeds.ac.uk/) was used throughout the work.

To explore the impact of hydrocarbons, oxygenates and peroxides on the calculated concentrations of OH and HO_2, four models, with different degrees of chemical complexity, were used. All the models were constrained to 15 min averages of measured concentrations of CO, CH_4, H_2, O_3, NO, NO_2, HCHO, selected NMHCs, H_2O and to measured temperature and photolysis rates (j(O^1D), j(NO_2), j(HONO), both channels of j(HCHO), j(CH_3COCH_3), j(CH_3CHO)). The NMHCs data were linearly interpolated to 15 min. The constraints of the different base models are shown in Table 3.

The 22 hydrocarbons were: ethane, propane, i-butane, n-butane, i-pentane, n-pentane, n-hexane, n-heptane, ethene, propene, acetylene, trans-2-butene, but-1-ene, i-butene, cis-2-butene, 1,3-butadiene, isoprene, benzene, toluene, ethylbenzene, m-xylene+p-xylene, o-xylene. The three oxygenates were acetaldehyde, methanol and acetone and the two peroxides were H_2O_2 and CH_3OOH (Lewis et al., 2005).

Model "fulloxyper" could be used only when enough peroxide data were available. The peroxides instrument was shut down on 30 August, so no data were available after that date. Even before 30 August peroxide concentrations, and in particular [CH_3OOH], were often below or close to the detection limit (0.02 ppb, Morgan and Jackson, 2002). There were differences between the results of the two sets of HCHO measurements (Still et al., 2005). The University of East Anglia (UEA) measurements were used to constrain the model, because they were made closer to the radical measurements location than was the Leeds instrument. HCHO measurements were not available after J233 (August 21), therefore the models for the following days could not be constrained to HCHO, which was instead calculated. Also, measurements of chloroform ($CHCl_3$) were not available before 3 August, so chloroform was included in the "full", "fulloxy" and "fulloxyper" models only after 3 August. SO_2, which was not measured, was set to a constant value of 55 ppt (Berresheim et al., 2002). Note that when the model was not constrained to the concentrations of oxygenates and hydroperoxides concentrations, these species were calculated as intermediates. The concentrations obtained were, for most species and especially those with longer lifetimes, more than an order of magnitude less than the measured concentrations, because of the importance of transport.

The wind profiler radar measurements indicated that a distinct diurnal cycle of the boundary layer (BL) was not always recognizable during NAMBLEX and often the synoptic pattern dominated over the local conditions (Norton et al., 2006). On many days during the campaign the boundary layer was roughly constant throughout the day with heights of 700–1500 m. On a few days, such as 9 August, the BL showed a diurnal variation with a height of 1000–1500 m during the day and 400–500 m during the night. The boundary layer height, however, did not influence significantly the modelled radicals.

Dry deposition terms were also included using the values of Derwent et al. (1996) except for peroxides (1.1 cm s^{-1} for H_2O_2 and 0.55 cm s^{-1} for organic peroxides), methyl and ethyl nitrate (1.1 cm s^{-1}) and HCHO (0.33 cm s^{-1}) (Brasseur et al., 1998). Dry deposition velocity for CH_3CHO and other aldehydes was assumed to be the same as that for HCHO. In the base models ("clean", "full", "fulloxy" and "fulloxyper"), heterogeneous uptake was calculated using Eq. (1) (Sect. 6) assuming irreversible loss of gas-phase species on aerosol.

Total OH loss due to CO, CH_4, H_2, hydrocarbons and oxygenates was calculated as $\sum_i k_{HC_i}[HC_i]$. Most of the time during NAMBLEX, with the exception of the semi-polluted days at the beginning of August, NMHCs accounted for only about 5–10% (average 7%) of the total OH loss. During the semi-polluted days their percentage increased up to ∼15% (Table 4). OH losses were dominated by CO, CH_4 and H_2 which together accounted for 60–80% of the total throughout the campaign.

Table 4 also shows the importance of oxygenated compounds as OH sinks. Acetaldehyde, formaldehyde, methanol and acetone taken together accounted for about 20% and up to 30% of the total OH losses. Acetaldehyde in particular was one of the major contributors to loss of OH (Table 4). Since oxygenates are also sources of radicals (Reactions R3–R4),

Table 3. Models used in this work.

Base models	Constraints	Heterogeneous uptake treatment	γ_{HO_2}	γ_{HOI}	γ_{HOBr}
"clean"	H_2, O_3, NO, NO_2, HCHO and H_2O, temperature, photolysis rates CO, CH_4	free-molecular expression	$1.40\times10^{-8}e^{(3780/T)}$ (a)	–	–
"full"	as "clean" + 22 hydrocarbons, DMS, chloroform	free-molecular expression	$1.40\times10^{-8}e^{(3780/T)}$ (a)	–	–
"fulloxy"	as "full" + 3 oxygenates	free-molecular expression	$1.40\times10^{-8}e^{(3780/T)}$ (a)	–	–
"fulloxyper"	as "fulloxy" + 2 peroxides	free-molecular expression	$1.40\times10^{-8}e^{(3780/T)}$ (a)	–	–
Improved models					
"fulloxy-io"	as "fulloxy" + IO, j(HOI)	free-molecular expression	$1.40\times10^{-8}e^{(3780/T)}$ (a)	0.6 (b)	–
"fulloxy-bro"	as "fulloxy" + BrO, j(HOBr)	free-molecular expression	$1.40\times10^{-8}e^{(3780/T)}$ (a)	–	0.6 (b)
"fulloxy-het"	as "fulloxy"	transition regime expression	$1.40\times10^{-8}e^{(3780/T)}$ (a)	–	–
"fulloxy-io-het"	as "fulloxy-io"	transition regime expression	$1.40\times10^{-8}e^{(3780/T)}$ (a)	0.6 (b)	–
"fulloxy-io-het_hoi"	as "fulloxy-io-het"	transition regime expression	$1.40\times10^{-8}e^{(3780/T)}$ (a)	0.06 (c)	-
"fulloxy-io-het_ho2"	as "fulloxy-io-het"	transition regime expression	1 (d)	0.6 (b)	–
"fulloxy-bro-het"	as "fulloxy-bro"	transition regime expression	$1.40\times10^{-8}e^{(3780/T)}$ (a)	–	0.6 (b)
"fulloxy-bro-het_hobr"	as "fulloxy-bro-het"	transition regime expression	$1.40\times10^{-8}e^{(3780/T)}$ (a)	–	0.06 (c)
"fulloxy-io_10x"	as "fulloxy-io" with [IO]×10	free-molecular expression	$1.40\times10^{-8}e^{(3780/T)}$ (a)	0.6 (b)	–
"fulloxy-bro-io"	as "fulloxy-bro" + IO, j(HOI)	free-molecular expression	$1.40\times10^{-8}e^{(3780/T)}$ (a)	0.6 (b)	0.6 (b)

(a) 0.006 at 298 K (Gratpanche et al., 1996).
(b) Wachsmuth et al. (2002).
(c) Mössinger and Cox (2001).
(d) maximum theoretical value.

it is important to accurately assess their impact on the radical budget. The sources and sinks of the oxygenated compounds during NAMBLEX are discussed in Lewis et al. (2005).

The modelling results were compared to OH and HO_2 measurements made during the day by laser-induced fluorescence (LIF) using the FAGE (Fluorescence Assay by Gas Expansion) approach (Smith et al., 2005). Two companion papers describe peroxy radical (HO_2 and HO_2+RO_2) chemistry during the day (Fleming et al., 2005) and night-time chemistry of HO_x and NO_3 (Sommariva et al., 2005[1]). A rigorous assessment of the model's uncertainty is very difficult owing to the large number of reactions and parameters involved. Using a simpler version of the model (similar to the "clean" model used in this work) a 2σ standard deviation of 30–40% for OH and 25–30% for HO_2 was estimated using a Monte Carlo technique coupled with Latin Hypercube Sampling (LHS) (Sommariva et al., 2004). The

[1]Sommariva, R., Ball, S. M., Bitter, M., Bloss, W. J., Fleming, Z. L., Heard, D. E., Jones, R. L., Lee, J. D., Monks, P. S., Pilling, M. J., Plane, J. M. C., and Saiz-Lopez, A.: Night-time radical chemistry during the NAMBLEX campaign, Atmos. Chem. Phys. Discuss., in preparation, 2005.

Table 4. Relative (%) OH loss due to CO, CH_4, H_2, NMHCs and oxygenates on some selected days during NAMBLEX (on 9 August H_2 was not measured and was estimated at 512 ppb; on 18 August CH_4, H_2 and CO were not measured and were estimated at 1835 ppb, 494 ppb and 85 ppb, respectively).

Measurements	1 Aug	9 Aug	15 Aug	18 Aug	21 Aug	31 Aug
CH_4+CO+H_2	61.3	66.3	65.5	60.2	64.1	81.3
$\sum$ oxygenates	25.1	27.0	28.0	28.3	22.6	12.3
$\sum$ alkanes	5.0	1.0	0.7	0.8	1.0	1.3
$\sum$ alkenes	3.1	2.2	2.6	2.6	3.8	2.7
$\sum$ dialkenes	2.3	2.1	0.4	3.8	6.9	0.5
$\sum$ aromatics	1.9	0.2	0.1	2.6	0.8	0.4
acetylene	0.2	0.1	0.1	0.1	0.1	0.2
DMS	1.2	1.1	2.7	1.5	0.8	1.3

model uncertainty is likely to be larger for the more complex models, but the uncertainties in the model input parameters are not sufficiently well defined to warrant a full uncertainty analysis. The 2σ standard deviation of the FAGE instrument during the NAMBLEX campaign was estimated as 44% for OH and about 50% for HO_2 (Smith et al., 2005).

5 OH and HO_2 with the base models

The results of the four base models are shown in Fig. 2 for OH and in Fig. 3 for HO_2 for several days during NAMBLEX together with the OH and HO_2 measurements by the FAGE technique.

The agreement for OH between the models and the measurements was within 25% on most days. 9 and 10 August were the two days which showed the best agreement with the models and measurements within 10% (Fig. 2a). 17–20 August corresponded to the period characterized by anticyclonic conditions and very slow wind speeds (<5 m/s), which caused air to stagnate over Mace Head. In these conditions the performance of the models was worse. On 17–19 August the OH concentration was overestimated by up to 50%. On 20 August the models underestimated the measurements by up to 30% (Fig. 2b). This is, however, within the combined uncertainties of the measurements and the estimated uncertainties of the model.

The comparison among the differently constrained models showed that the "clean" model always calculated higher [OH] than the models with additional constraints. In fact, for all the modelled days the best agreement was obtained with the "fulloxy" and the "fulloxyper" models which included constraints to the measured concentrations of the oxygenated compounds (methanol, acetaldehyde and acetone). Reactions with these compounds represent important losses for OH (Table 4), but they were also radical sources through their photolysis. When the model was constrained to measured oxygenates, modelled [OH] was lower than when the

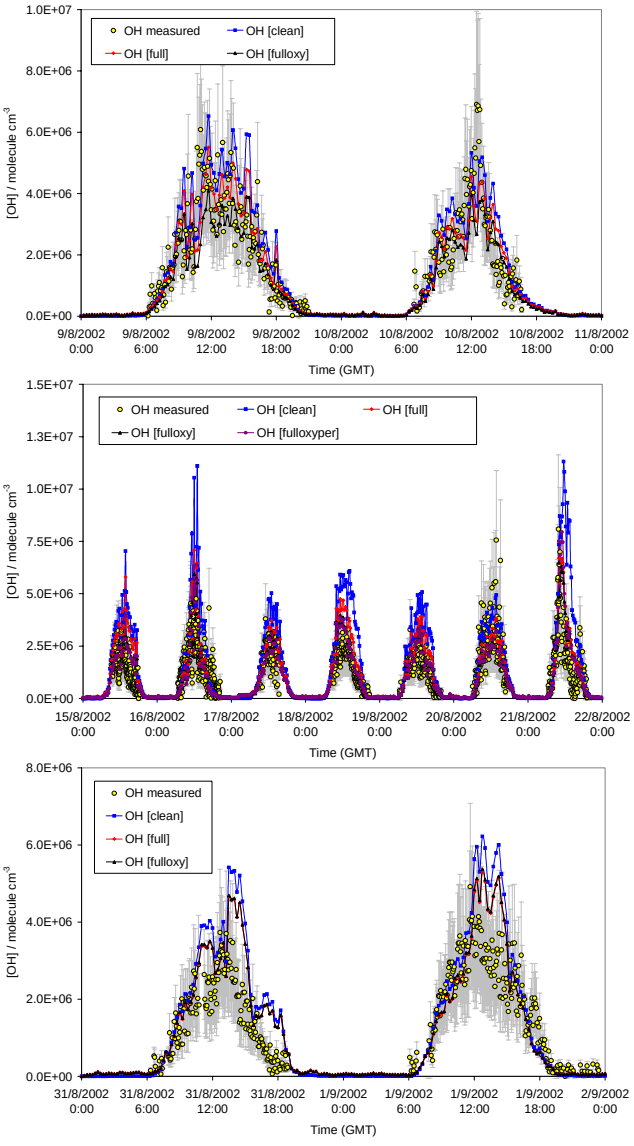

Fig. 2. Model-measurement comparison for OH with the base models. **(a)** 9–10 August, **(b)** 15–21 August, **(c)** 31 August–1 September. The measurements 2σ standard deviation is shown in grey.

model was not constrained to the oxygenates, showing that these species acted as net sinks for OH. The difference between the "fulloxy" and the "fulloxyper" models appeared to be negligible, showing that constraining the model to peroxides (H_2O_2 and CH_3OOH) did not have a significant impact on modelled [HO_x].

In contrast to previous campaigns, e.g. SOAPEX-2 (Sommariva et al., 2004), the models reproduced reasonably well the shape of the OH profiles and they followed closely the increase of [OH] at sunrise and the decrease at sunset, possibly owing to measured photolysis rates other than j(O^1D) and j(NO_2) during NAMBLEX. The agreement with the measured profile is particularly good on 9 and 10 August

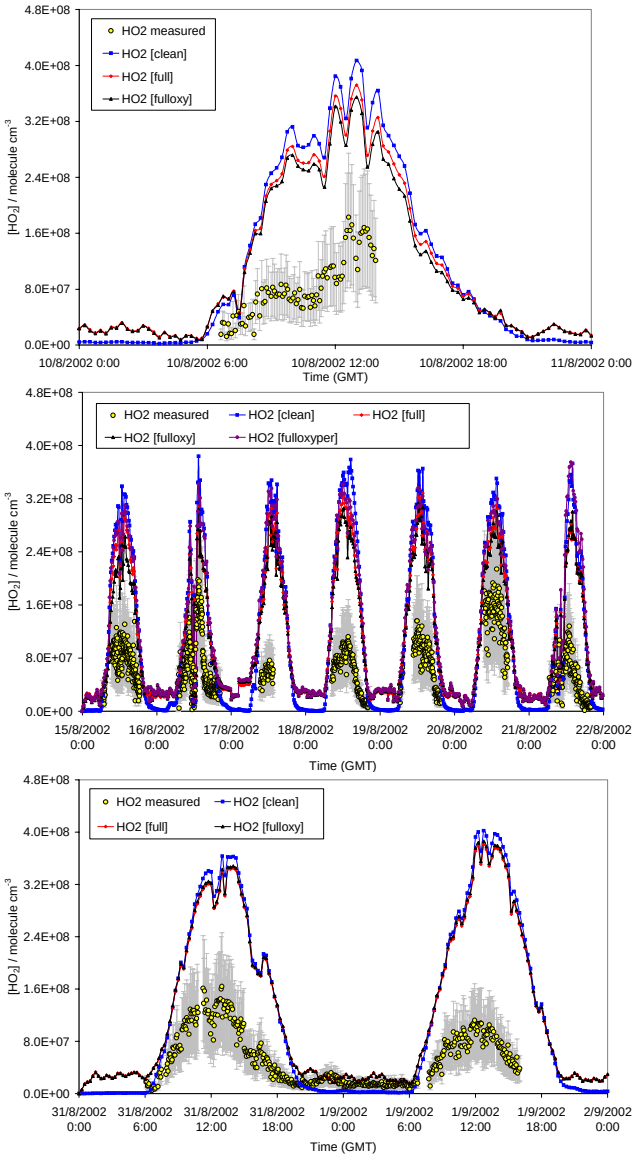

Fig. 3. Model-measurement comparison for HO_2 with the base models. **(a)** 10 August, **(b)** 15–21 August, **(c)** 31 August–1 September. The measurements 2σ standard deviation is shown in grey.

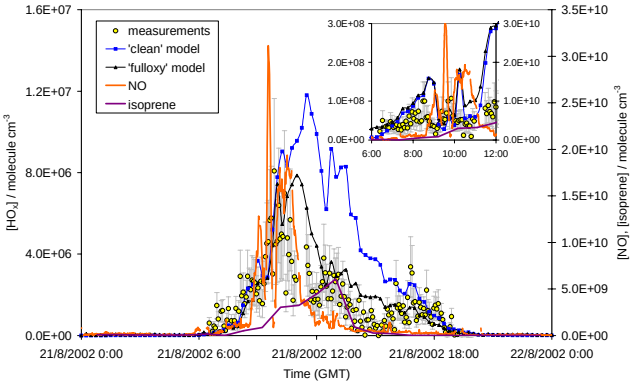

Fig. 4. Model-measurement comparison for OH with the base models and measured concentrations of NO and isoprene (21 August). HO_2 during the morning of 21 August is shown in the inset. The measurements 2σ standard deviation is shown in grey.

(Fig. 2a), which were also the two days with the best agreement with the measurements.

Despite technical difficulties at the beginning of the campaign with the FAGE instrument, there were many days of HO_2 measurements during NAMBLEX. The results of the models are shown together with the measurements in Fig. 3. Data for 10 August had a larger uncertainty, because this was the first day of the campaign that the HO_2 cell of the instrument was working. HO_2 data for the following days were considered more reliable.

The agreement between modelled and measured [HO_2] was not as good as for OH. The models overestimated the concentration of HO_2 on all the modelled days by at least a factor of 2. This is in agreement with the model results of previous campaigns in the marine boundary layer, e.g. Sommariva et al. (2004) for Cape Grim, despite a considerable improvement of the model performance with respect to OH. This suggests that some important part of the mechanism is either missing or badly implemented, because the discrepancy between the model and the measurements appear to be independent from the chemical and physical conditions, which in Mace Head and in Cape Grim were different even during the clean periods.

A test run was made by changing the rate coefficient of the reaction HO_2+HO_2 to test the sensitivity of the model to the kinetic parameters of the HO_2 self-reaction. In the low NO_x conditions encountered in Mace Head this was one of the dominant loss pathways of HO_2 (Sect. 8). The model showed that increasing $k_{HO_2+HO_2}$ by 50% resulted in a decrease of [HO_2] by only 10–15% due to radical cycling which buffered the effect of increased HO_2 loss via this route.

The models were also run using the Leeds HCHO dataset instead of the UEA one. The Leeds data were consistently higher than the UEA data (Still et al., 2005), but this had a negligible influence on the calculated [OH] and increased calculated [HO_2] by at most 15%.

The model was able to reproduce the impact on [HO_2] of the NO events on 16 and 21 August (Figs. 3b and 4). On these two occasions, strong spikes of NO of up to 2.5×10^{10} molecule cm^{-3} were detected by the NO_{xy} instrument. The source of these spikes is unknown. It probably was a local source, such as a car or a ship, characterized by a strong but short burst of NO_x. During these events, HO_2 suddenly decreased while OH increased because of the reaction with NO which accelerated the HO_x cycle (Fig. 4). In particular, during the morning of 21 August, between 09:00 and 12:00, two large peaks of NO of up to 1.5×10^{10} molecule cm^{-3} were detected. Figure 4 shows that measured and modelled HO_2 increased in the early morning, following the increase in the

radical production by photolysis and then was suddenly depleted during the first NO event, rose as NO returned to "normal" levels and was depleted again during the second NO event, before returning to its normal level around midday. The same happened to the peroxy radicals, while, at the same time, both measured and modelled OH showed a large increase. This was clearly due to the reactions of peroxy radicals (HO_2 and RO_2) with NO. It is interesting to note that, even though the model overestimated [HO_2] by a factor of 2 or more, it was able to correctly reproduce the behaviour of the HO_x radicals during these pollution events. This suggests that the mechanism works better at higher NO_x conditions, which may indicate that the problem lies mainly in the treatment of the peroxy-peroxy reactions.

The agreement between the models constrained to the hydrocarbons ("full", "fulloxy" and "fulloxyper") and the CO-CH_4 model ("clean") was generally quite close on most of the modelled days, both for OH and for HO_2 (Figs. 2–3). This is because for most of the time the NMHCs only accounted for about 7–10% of the total OH loss (Table 4) and therefore the great part of the OH chemistry was driven by CO, CH_4 and H_2 (up to 70% of the total OH loss) which were common to all the four models. The only notable exception was on 21 August when, starting from mid-morning, the concentration of OH calculated with the "clean" model was up to a factor of 3 higher than the concentration calculated with the "fulloxy" model (Fig. 4). However, this was not the case for modelled [HO_2], whose concentrations calculated with both the "clean" and the "fulloxy" models agreed to within 10%.

This discrepancy was due to isoprene, which was not included in the "clean" model. A very strong isoprene peak with a maximum of 6×10^9 molecule cm^{-3} was detected shortly after midday on 21 August. Figure 4 shows that in the first part of the morning the two models agreed to within 5% and they started to diverge as the isoprene concentration grew. Isoprene reacts very quickly with OH and on this day it accounted for about 7% of the total OH losses (24 h average; Table 4). Also, isoprene produces formaldehyde (Carslaw et al., 2000), which is itself an important OH co-reactant and HO_2 source.

In the "fulloxy" model, around midday, isoprene was the most important OH loss (2.2×10^6 molecule cm^{-3} s^{-1}), followed by HCHO and CO (1.4×10^6 and 1.9×10^6 molecule cm^{-3} s^{-1}, respectively). By contrast, in the "clean" model isoprene was absent and OH was lost mainly to reaction with CO and CH_4, while the rate of reaction with HCHO was only about one third of CO. At the same time (12:00) HO_2 production in the "fulloxy" model was dominated by HCHO oxidation (2.5×10^6 molecule cm^{-3} s^{-1}), which was faster than the reaction of OH with CO (1.9×10^6 molecule cm^{-3} s^{-1}); the decomposition of the isoprene derived alkoxy radicals was also significant (1.4×10^6 molecule cm^{-3} s^{-1}). In the "clean" model, the rate of production of HO_2 via OH+HCHO was only about one third of the rate of production via OH+CO. Formaldehyde chemistry was much more significant in the "fulloxy" model than in the "clean" model and it is reasonable to conclude that this was related to isoprene oxidation.

It is therefore likely that the agreement between the "clean" and the "fulloxy" models with respect to the modelled [HO_2] was just a consequence of counterbalancing chemistry: isoprene oxidation caused OH to be destroyed and HO_2 to be produced in the "fulloxy" model and this resulted in an increase in HO_2 production which brought it close to the values predicted by the "clean" model. It is important to note that this was possible only because of the extremely low concentration of NO_x ($<5.1\times10^8$ molecule cm^{-3}) at the time when isoprene reached its maximum concentration. In these conditions the production of OH from HO_2 (via NO and O_3) steadily decreased through the day, so that the recycling between HO_2 and OH slowed down, allowing the buildup of HO_2.

21 August had another interesting feature: a short burst of radicals in the late afternoon (Fig. 4). The increase in OH in the late afternoon, around 18:00, was related to a sharp increase in the ozone photolysis rates. A similar sharp increase in the photolysis rates also occurred on 9, 15, 17 and 31 August and 1 September. Fleming et al. (2005) have suggested that the increase was due to the reflection of sunlight from the bottom of the clouds at high SZA. The modelled profile for [OH] on 31 August (Fig. 2c) is quite broad and extends over ca. 2 h. That for HO_2 is much narrower and is centered on the photolysis spike at 16:30 (Fig. 3c). This difference arises because of a sharp increase in NO at 18:00 that sustained modelled [OH] at the expense of modelled [HO_2]. No similar increases were observed in the measured radical concentrations.

6 Halogens and heterogeneous uptake

The comparisons between the measurements and the base model results were satisfactory, within the combined uncertainties of the model and of the measurements, for OH, but not for HO_2. Several hypothesis have been suggested in previous studies to explain the difference between modelled and measured HO_x, with particular regard to HO_2. In this section, reactions of halogen monoxides and heterogeneous uptake of radicals will be discussed as possible explanations for the observed discrepancies using the extensive dataset of measurements collected during NAMBLEX.

Halogen chemistry has long been known to affect tropospheric chemistry in different ways (Chameides and Davies, 1980; Davis et al., 1996; Carpenter, 2003). Recent observations of the halogen oxides IO, OIO and BrO suggested that their reactions can be very important in the marine boundary layer chemistry (Alicke et al., 1999; Allan et al., 2000). In particular, Kanaya et al. (2002) suggested that comparatively high values of IO (up to 25 ppt) could explain the

overestimation of measured HO_2 by up to 70%. However, prior to NAMBLEX, lack of simultaneous measurements of halogen monoxides (XO), HO_x and other related species did not allow a complete evaluation of the impact of these species on $[HO_x]$.

During NAMBLEX, IO and BrO were measured with the DOAS technique (Saiz-Lopez and Plane, 2004; Saiz-Lopez et al., 2004, 2005). IO was measured on several days during the campaign and typically showed a diurnal cycle clearly anti-correlated with tidal height (Saiz-Lopez et al., 2005). In particular, during the week from 15 to 21 August, IO was measured every day, with a maximum concentration of 4 ppt (hourly average). BrO was measured on six days (1, 3, 4, 10, 31 August and 1 September) with a maximum concentration of 6.5 ppt and an average concentration of 2.3 ppt. The diurnal profile was characterized by a short-lived pulse after dawn, followed by a maximum in the afternoon. The detection limit was 0.5 ppt for IO and 0.8 ppt for BrO (Saiz-Lopez and Plane, 2004; Saiz-Lopez et al., 2004). Unfortunately, since the two compounds were monitored in different spectral regions (IO: 415–450 nm, BrO: 320–360 nm) they could not be measured simultaneously.

The halogen monoxides directly affect OH and HO_2 concentrations in the troposphere mainly via the reaction with HO_2, followed by photolysis or heterogeneous uptake of HOX (where X=I, Br), thus providing a sink for HO_2 and a route for $HO_2 \rightarrow OH$ conversion (Reactions R5–R6–R7).

$$XO + HO_2 \rightarrow HOX + O_2 \quad \text{(R5)}$$

$$HOX + h\nu \rightarrow OH + X \quad \text{(R6)}$$

$$HOX + \text{aerosol} \rightarrow \quad \text{(R7)}$$

Uptake of HOX upon aerosol leads to loss of HO_x from the gas-phase system (Carpenter, 2003; McFiggans et al., 2000). In unpolluted conditions, if levels of IO or BrO are sufficiently high, Reactions (R5–R6–R7) will affect HO_x abundance and partitioning. Halogen oxides also impact O_3 loss and NO_x partitioning, thus indirectly affecting HO_x. However, in this work, these were implicitly included in the model, which was constrained to measured O_3 and NO_x.

Previous work showed that higher aerosol surface areas and HO_2 uptake coefficients (γ) could have a large impact on $[HO_2]$, without affecting [OH] too much, due to the slow recycling in unpolluted conditions (Sommariva et al., 2004; Haggerstone et al., 2005). However, there is substantial uncertainty about the effect of aerosol uptake on OH and HO_2 concentrations, mainly due to a lack of ancillary aerosol data recorded during many of the recent MBL campaigns (Carslaw et al., 1999; Kanaya et al., 2000, 2001).

The aerosol uptake in the base models was calculated with the free-molecular expression:

$$k_{\text{het}} = \frac{A\bar{v}\gamma}{4} \quad (1)$$

where A is the total aerosol surface area, $\bar{v}$ is the mean molecular speed and γ is the temperature dependent gas/surface reaction probability (uptake coefficient). One of the most important improvements of the NAMBLEX campaign over previous campaigns was the availability of detailed measurements on the chemical and physical properties of particles. Using these data more precise rate coefficients for the uptake of the relevant species on aerosol particles could be calculated using the transition regime expression (Eq. 2) (Sander, 1999), which accommodates the transition between gas-phase diffusion control and uptake control:

$$\begin{aligned} L\bar{k_{mt}} &= \int_0^\infty \left(\frac{dV(r)}{dr} \times k_{mt}(r) \right) dr \quad (2) \\ &= \int_0^\infty \left(\frac{4}{3}\pi r^3 \frac{dN(r)}{dr} \times \left(\frac{r^2}{3D_g} + \frac{4r}{3\bar{v}\alpha} \right)^{-1} \right) dr \end{aligned}$$

where r is the droplet radius, D_g is the gas-phase diffusivity, α is the mass accommodation coefficient, $\bar{v}$ is the mean molecular speed and $N(r)$ and $V(r)$ are the number density and the volume of particles with radius smaller than r (Sander, 1999). Equation (2) is the product of total aerosol volume (L) for the mass transfer coefficient ($\bar{k_{mt}}$), averaged over the entire particle size range. The mass transfer coefficient has two components: one describing the gas-phase diffusion to a spherical droplet, which depends on the diffusivity of the molecule (D_g) and the other describing the transfer of the molecule to the liquid-phase, which depends on the mass accommodation coefficient of the molecule (α). Depending on the conditions, the species, the aerosol characteristics and the mass accommodation coefficient of the species, the uptake rate can be controlled either by the diffusion or by the uptake or by both processes. When the system is diffusion limited, it is less sensitive to α so the large uncertainties in α for many species have a much smaller impact (Sander, 1999).

It must be noted that this treatment of the heterogeneous uptake of gas-phase species is not yet completely adequate. First, it considers only in part the effect of the chemical composition of the particles, which is likely to be important. For example, Bates et al. (1998, 2001) measured strong variations in the chemical composition of the Aitken, accommodation and sea-salt dominated coarse modes that would influence the radical uptake rates, particularly the extent of aerosol acidification. Secondly, it does not take into account the reactivity of the species inside the particle and the release of compounds from the particles into the gas-phase. The uptake rates for HO_2, HOX and other relevant species were calculated with the procedure explained in Haggerstone et al. (2005) using measurements by a Differential Mobility Particle Sizing system (3–750 nm), a GRIMM Optical Particle Counter (450 nm–6.5 µm) and a Forward Scattering Spectrometer Probe (1–20 µm) (Coe et al., 2005). The binary diffusion coefficients for HO_2 and HOX were calculated using

the molecular mass of HOI. This simplification did not introduce a significant error in the calculations because the equation used to calculate D_g is much more sensitive to the effective diameter of the molecules (Eq. 4 in Coe et al., 2005).

In this work it was assumed that gas-phase species are instantaneously lost after being taken up on aerosol, therefore the uptake coefficient (γ) was used in Eq. (2) instead of the mass accommodation coefficient (α). Also, it was assumed that all particles were sea-salt particles, which under the unpolluted conditions of most of the modelled days is reasonable (Coe et al., 2005).

The "clean", "full", "fulloxy" and "fulloxyper" models were modified by adding the simple mechanism in R5–R6–R7 and/or constraining them to the heterogenous uptake rates calculated with Eq. (2). The rate coefficients for the reactions of XO with HO_2 were $k_{IO+HO_2}=1.4\times10^{-11}\exp(554/T)$ (Knight and Crowley, 2001) and $k_{BrO+HO_2}=3.8\times10^{-12}\exp(540/T)$ (Bloss et al., 2002; DeMore et al., 2003). The photolysis rates of HOX were calculated from the spectral radiometer data using cross sections from Bauer et al. (1998) for HOI and Ingham et al. (1998) for HOBr.

The uptake coefficient of HO_2 was set to $1.40\times10^{-8}e^{(3780/T)}$ (0.006 at 298 K, Gratpanche et al., 1996) and then changed to 1.0 (maximum theoretical value) as the "upper limit case" (Table 3). In this way the whole range of γ_{HO_2} could be explored to examine the sensitivity of modelled HO_2 to this parameter. In the models containing the halogen monoxide mechanism the uptake coefficients of HOI and HOBr were very important, as they determined the impact that iodine and bromine chemistry had upon OH concentration. Both uptake coefficients were set to 0.6 (Wachsmuth et al., 2002) and then changed to 0.06 as "lower limit case" (Mössinger and Cox, 2001) to check the effect of a smaller heterogeneous loss of these species on the radical balance (Table 3).

The improved models were used on the central week of NAMBLEX, from the 15 to 20 August. During this period OH, HO_2 and total peroxy radicals were measured every day and IO and aerosol data were available. The impact of BrO was tested on another day (31 August), as the two halogen oxides were not measured at the same time. The constraints of the improved models are shown in Table 3.

7 OH and HO_2 with the improved models

The results of the improved models are shown in Figs. 5 and 6, together with the measurements of HO_x radicals. 18 August was the most significant day, because the concentration of IO was the highest measured during the campaign, peaking at 4 ppt. Most of the following discussion will therefore concentrate on this day. The model results shown in these figures are from the "fulloxy" model. However, the effect of implementing a different treatment for the heterogeneous uptake process and of adding a halogen mechanism was comparable for all the models. This is expected, because they affect elements of the mechanism which are common to all the four models.

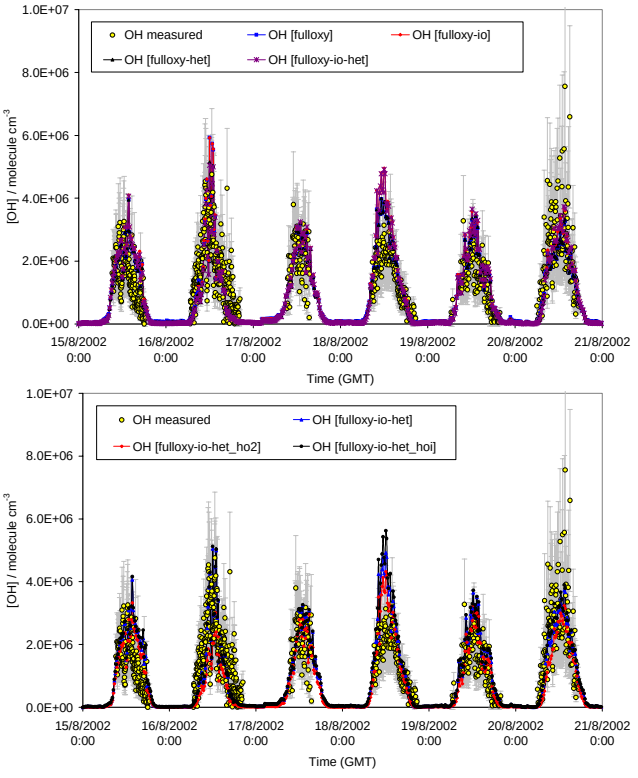

Fig. 5. Model-measurement comparison for OH with the improved models (15–20 August). **(a)** Showing the impact of IO and of the transition regime expression, **(b)** showing the effect of changing the uptake coefficients of HOI and HO_2. The measurements 2σ standard deviation is shown in grey.

Figure 5a shows that modelled OH was not affected very much by the model improvements. The photolysis of HOI had a limited impact on [OH]. On the day with the highest IO concentration (18 August), [OH] increased by at most 15% with respect to the base model. Given that the uncertainty of the model was estimated to be up to 40%, comparable to the measurements uncertainty (Sommariva et al., 2004), a variation of 15% did not significantly change the agreement with the measurements for OH. Moreover, the fine structure and the profile of OH was unchanged by inclusion of IO chemistry. This was also expected, because IO had a diurnal profile with higher concentration around midday and in the first part of the afternoon, so that its inclusion did not change the radical balance in the early morning and late afternoon and mainly affected HO_x in the central part of the day. The impact of HOI on OH depends on the partitioning of HOI between photolysis and heterogeneous loss. In the first run (Fig. 5a) γ_{HOI} was set to a value of 0.6 (models "fulloxy-io" and "fulloxy-io-het"). Decreasing γ_{HOI} increased the amount

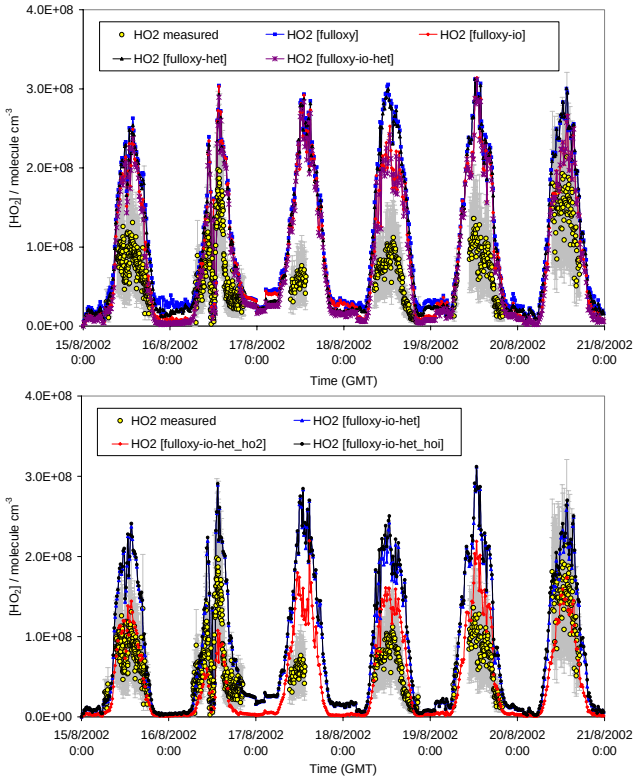

Fig. 6. Model-measurement comparison for HO_2 with the improved models (15–20 August). **(a)** Showing the impact of IO and of the transition regime expression, **(b)** showing the effect of changing the uptake coefficients of HOI and HO_2. The measurements 2σ standard deviation is shown in grey.

of HOI, which was photolyzed resulting in a higher calculated [OH]. Figure 5b shows that the model which used uptake rate coefficients with γ_{HOI}=0.06 ("fulloxy-io-het_hoi") calculated a concentration of OH 10–15% higher than that calculated with γ_{HOI}=0.6 (model "fulloxy-io-het").

The use of a treatment for the aerosol uptake based upon the measurements barely affected the modelled OH concentration, mainly because most OH sources and sinks are not lost upon the particles. Uptake of HONO can increase the effectiveness of reaction with NO as an OH sink. Normally, under daylight conditions HONO photolyzes to regenerate OH, but uptake could reduce [HONO] and hence the rate of regeneration. Under the conditions considered, however, [NO] was too small to make this an important reaction. The main impact on OH is likely to be through HO_2 uptake on aerosol, reducing the rate of OH production via HO_2+NO. In the first run (Fig. 5a) γ_{HO_2} was set to a very low value (0.006 at 298 K). In this case HO_2 uptake was limited by the mass accommodation process rather than by the gas-phase diffusion. Figure 5b shows the change in modelled [OH] when the uptake coefficient of HO_2 was set to the maximum theoretical limit of 1.0 (model "fulloxy-io-het_ho2"). Modelled OH decreased, because there was a net loss of radicals via the removal of HO_2 from the system. This effectively balanced the increase due to HOI photolysis, so that the best agreement between modelled and measured OH was achieved with a model containing IO chemistry and a detailed treatment of aerosol uptake using the values of 1.0 and 0.6 for the uptake coefficients of HO_2 and HOI, respectively.

The largest impact of the improvements to the models was on HO_2, which directly reacts with IO and whose rate of loss on the aerosol is much faster than the rate of loss of the other radicals (like OH and CH_3O_2). Figure 6 shows the results of the improved models compared to the "fulloxy" base model and the results of the test runs with different uptake coefficients (γ) for HOI and HO_2.

The reaction with IO accounted for a large fraction of the total HO_2 losses (Sect. 8), resulting in a significant decrease of modelled HO_2 through Reaction (R5). The impact of IO obviously depended on the concentration of IO and was therefore maximum on 18 August when IO was about 4 ppt. On this day modelled HO_2 decreased by up to 30% (models "fulloxy-io" and "fulloxy-io-het"), which was, however, not enough to bring modelled [HO_2] close to the measurements (Fig. 6a).

When the uptake coefficient of HOI was decreased by a factor of 10 (from 0.6 to 0.06), the concentration of HO_2 slightly increased (model "fulloxy-io-het_hoi"), because of the resulting increase in [OH] from increased photolysis of HOI (Fig. 6b).

With γ_{HO_2}=0.006 (at 298 K) the use of the transition regime expression (model "fulloxy-het" and "fulloxy-io-het") instead of the free-molecular expression (model "fulloxy" and "fulloxy-io") to describe the heterogeneous uptake did not cause a significant change in the concentration of HO_2, due to the low value of the uptake coefficient. Under these conditions, the uptake of HO_2 on the particles is limited by the accommodation process. In Figs. 6a and 7b, the slight decrease in modelled [HO_2] (a few percent between 15 and 21 August and less than 10% on 31 August with respect to the base model) was due to higher γ_{HCHO} in the improved models which resulted in a faster removal of HCHO and, hence, of HO_2.

For γ_{HO_2}=1.0 (which is the maximum theoretical limit of the uptake coefficient) the modelled concentration of HO_2 dramatically decreased (model "fulloxy-io-het_ho2"). The results are shown in Fig. 6b. On certain days, such as 15 and 20 August, HO_2 was reduced by up to 40%, reaching good agreement with the measurements. On one day (16 August) the decrease in HO_2 concentration was too large and the model underestimated the measurements by up to 50%. In the central days of the week (17, 18 and 19 August), despite the decrease in modelled [HO_2], the model still overestimated the measurements by up to 30%.

HO_2 was also measured during the night between 31 August and 1 September (Smith et al., 2005). The choice of the treatment to describe heterogeneous uptake (free-molecular vs. transition regime expressions) had similar impacts on

calculated [HO_2] during the day and during the night. However, since the agreement between the model and the measurements was better during the night than during the day (within 30%), [HO_2] was underestimated by up to an order of magnitude when γ_{HO_2}=1. The comparison between the models and the measurements and the discussion of HO_2 chemistry during the night can be found in Sommariva et al. (2005)[1].

The impact of BrO on OH and HO_2 is shown in Fig. 7 on 31 August, one of the few days of NAMBLEX on which BrO was measured. While IO chemistry had the effect of increasing [OH], BrO decreased it by about 10%, when using the free-molecular expression (model "fulloxy-bro"), and by up to 20%, when using the transition regime expression, (model "fulloxy-bro-het" with γ_{HOBr}=0.6). The different impact of BrO on OH was due to the fact that HOBr photolysis rate is about 4.5 times slower than the HOI photolysis rate, meaning that the aerosol was a more important sink for HOBr than for HOI. It also means that [OH] was more sensitive to changes in the uptake coefficient of HOBr than of HOI. This is consistent with the fact that when γ_{HOBr} was set to 0.06 (model "fulloxy-bro-het_hobr") the modelled [OH] increased with respect to the model with γ_{HOBr}=0.6 (Fig. 7a). With less HOBr lost on the particles, because of the lower uptake coefficient, and more photolyzed to OH, the magnitude of the radical sink was lower.

The effect of BrO on [HO_2] was similar to that of IO, as both radicals consume HO_2, producing HOX. A decrease of up to 25% in modelled [HO_2] could be observed when the model was constrained to measured BrO (model "fulloxy-bro"). The use of the transition regime expression to describe the heterogeneous uptake had a higher effect when the model contained bromine chemistry (model "fulloxy-bro-het") than when it contained iodine chemistry (model "fulloxy-io-het" in Fig. 6), because the model was more sensitive to the uptake rate of HOBr. The impact of BrO on modelled HO_2 was lower when γ_{HOBr} was set to a value an order of magnitude lower (0.06 in model "fulloxy-bro-het_hobr" instead of 0.6 in model "fulloxy-bro-het", Fig. 7b). This is because less HOBr was taken up on aerosol and more was photolyzed, producing OH which in turn produced HO_2, thus buffering the loss of HO_2 caused by the reaction HO_2+BrO.

These results can be compared with a similar study by Kanaya et al. (2002) from a field campaign at Rishiri Island, in Northern Japan. Their model overestimated HO_2 by up to 70% and underestimated OH, particularly during the low NO_x periods. The model was modified to include an iodine source and a simple halogen mechanism (about 30 reactions). The source of iodine was assumed to be CH_2I_2, which was measured at the same site during another field campaign (0.4 ppt on average) and was considered to represent all the other iodocarbons. The concentration of CH_2I_2 was kept constant during the day and varied in several runs between 0.3 and 1 ppt. Under their assumptions a concentration of 25 ppt of IO was necessary to achieve better agreement between modelled and measured [HO_2], without considering the loss of HOI on the particles. With γ=0.5, which is a value similar to the one used in this work, up to 12 ppt of IO were necessary. Kanaya et al. (2002) also tested the model using an increased uptake rate of HO_2 (with γ=0.5), but the decrease in modelled [HO_2] was not enough to reach agreement with the measurements. The reactivity of HO_2 with BrO was considered as well, but since the rate coefficient is about 3 times lower than the rate coefficient of the reaction with IO, Kanaya et al. (2002) concluded that BrO could not play a significant role in HO_2 chemistry as it was improbable that its concentration was 3 times higher than IO.

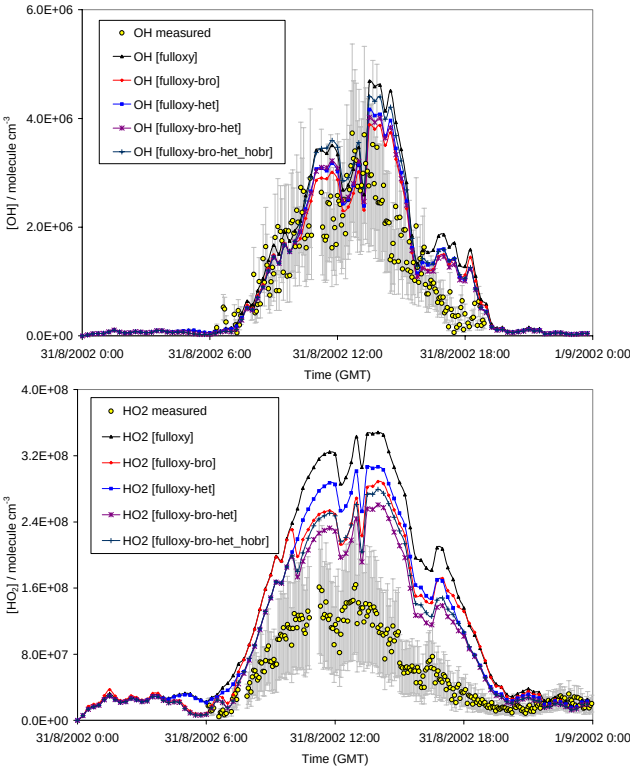

Fig. 7. Model-measurement comparison with the improved models (31 August). **(a)** OH, **(b)** HO_2. The measurements 2σ standard deviation is shown in grey.

During NAMBLEX BrO was on average present at higher concentrations than IO, though not by a factor of 3 (maximum concentrations at Mace Head were 4 ppt and 6.5 ppt, respectively). However the results of this study show that both IO and BrO have a significant impact on [HO_x], although this is heavily dependant on the uptake coefficients used for HOX and HO_2.

A very important issue is the spatial distribution of IO. The concentration measured by the DOAS is the mean value along the instrument light path (4.2 km), so if the emissions of halocarbons and/or molecular iodine are higher near the shore, the concentration of IO at the measurements site might be substantially higher than the DOAS measurements and the

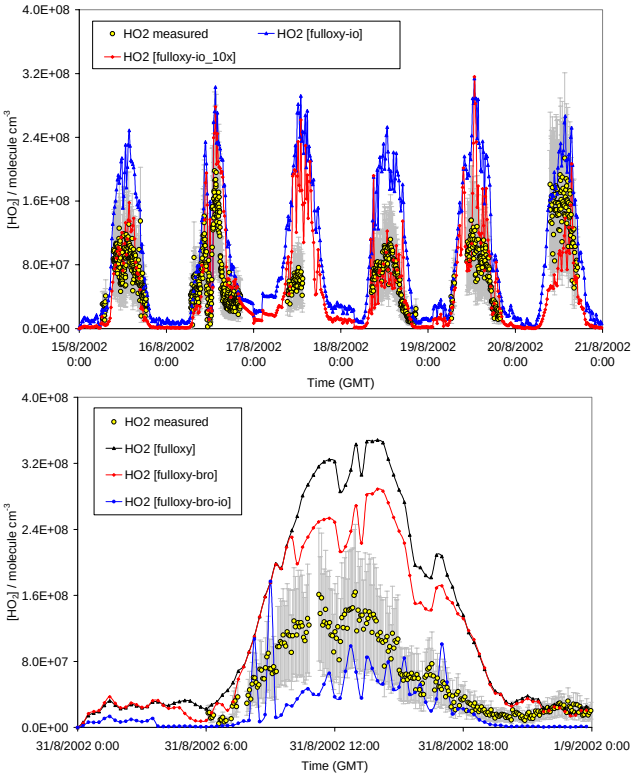

Fig. 8. Model-measurement comparison for HO_2 with the improved models. **(a)** Models constrained to different concentrations of IO (15–20 August), **(b)** models constrained to estimated IO and measured BrO (30 August). The measurements 2σ standard deviation is shown in grey.

impact on [HO_2] much higher than estimated above. A modelling study reported in this issue (Saiz-Lopez et al., 2006) investigated the relative concentrations of IO and I_2, observed at Mace Head during NAMBLEX. The model showed that the ratio of IO to I_2 in the DOAS beam (∼1:2) could only be explained if I_2 and IO were concentrated in a small fraction of the DOAS path (in the intertidal zones, about 160 m at each end of the light path), due to I_2 release from exposed macro-algae (Saiz-Lopez et al., 2006). From the model calculation, [I_2] should be of the order of 100 ppt (confirmed using in situ measurements by broadband cavity ring-down spectroscopy and by inductively coupled plasma-mass spectrometry), which implies [IO] of the order of 50 ppt, about an order of magnitude higher than the DOAS measurements, assuming a homogeneous distribution (Saiz-Lopez et al., 2006).

To test this hypothesis, the "fulloxy-io" model was run with iodine chemistry, using a concentration of IO ten times higher than assuming homogeneity, as used in the calculations above. The heterogeneous uptake of HOI was calculated with the free-molecular expression (Eq. 1) using γ_{HOI}=0.6 and γ_{HO_2}=0.006. The results for HO_2 are shown in Fig. 8a. Modelled HO_2 decreased by up to 50% resulting in such a high concentration of IO that photolysis of HOI was the dominant process converting HO_2 to OH (more than an order of magnitude faster than via the reaction with NO) and this resulted in an increase in modelled OH by up to 30%. The agreement with OH measurements still remained reasonably good on most of the days and actually improved on 20 August, the only day when the base model underestimated OH (Fig. 5a). If this was the case, and the concentration of IO at the site was an order of magnitude higher than the DOAS measurements, iodine chemistry would dominate the HO_x budget.

Another important issue is the simultaneous presence of IO and BrO in the MBL. The two species could not be measured at the same time, but they are likely to be present at the same time, though with different spatial distribution (Saiz-Lopez and Plane, 2004; Saiz-Lopez et al., 2004). The joint impact of IO and BrO on radicals concentration was simulated using measured BrO on 31 August and setting IO to the levels measured on 18 August. The results for HO_2 are shown in Fig. 8b. The modelled concentration of HO_2 decreased by more than a factor of 4, with respect to the base model and more than a factor of 3 with respect to the model constrained only to BrO, leading to a large underestimation of measured HO_2. On the other hand OH was increased by up to 30% with respect to the base model, due to the faster photolysis of HOI. It must be stressed that this is a quite rough estimate, because IO was not measured on this day and the concentration used was the highest measured during the campaign.

8 Analysis of the improved models

The impact of IO and BrO on [HO_x] was more evident on 18 August and 31 August, respectively, when the measured concentrations of the two halogen species was higher. Therefore on these two days a rate of production and destruction analysis of the models was carried on to understand the exact role played by these species in the radical processes. The analysis was done on the models containing halogen chemistry and using the transition regime expression to describe the heterogeneous uptake ("fulloxy-io-het" and "fulloxy-bro-het" models, with γ_{HOI}=0.6 and γ_{HO_2}=0.006). The results are summarized in Fig. 9 for OH and in Fig. 10 for HO_2.

The main source of OH was the photolysis of ozone, followed by the reaction of HO_2 with NO and by the reaction of HO_2+O_3 (Fig. 9). On 18 August the photolysis of HOI was most of the time a more important source of OH than HO_2+NO (up to 2×10^6 vs. 1.3×10^6 molecule cm^{-3} s^{-1}). This explains why the introduction of iodine chemistry in the model had such a large effect on modelled [OH] (Sect. 6). On most of the other days in NAMBLEX HOI photolysis was probably less important as a source of OH, because the concentration of IO was lower, but it is still expected to be significant. On 31 August, the photolysis of HOBr

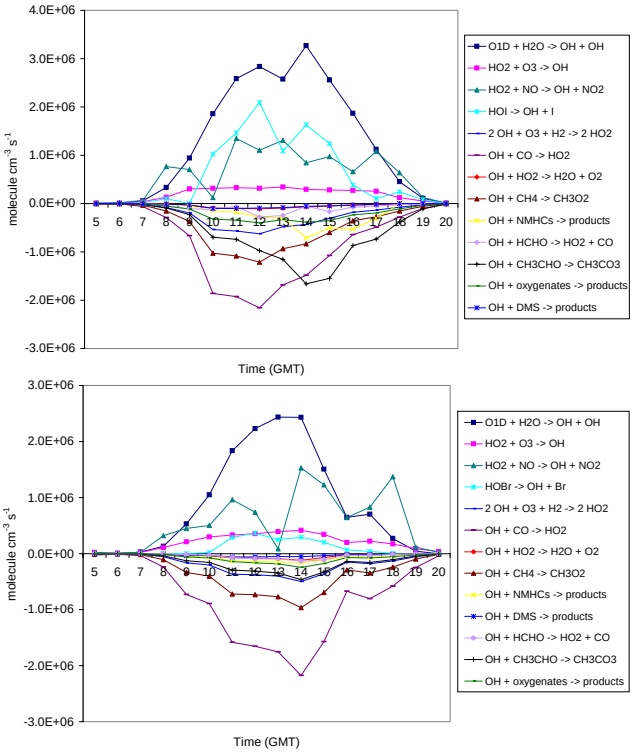

Fig. 9. Rates of production and destruction of OH. **(a)** 18 August ("fulloxy-io-het" model), **(b)** 31 August ("fulloxy-bro-het" model). 2 $OH+O_3+H_2 \rightarrow 2\ HO_2$ indicates the sum of the rates of $OH+O_3 \rightarrow HO_2$ and $OH+H_2 \rightarrow HO_2$.

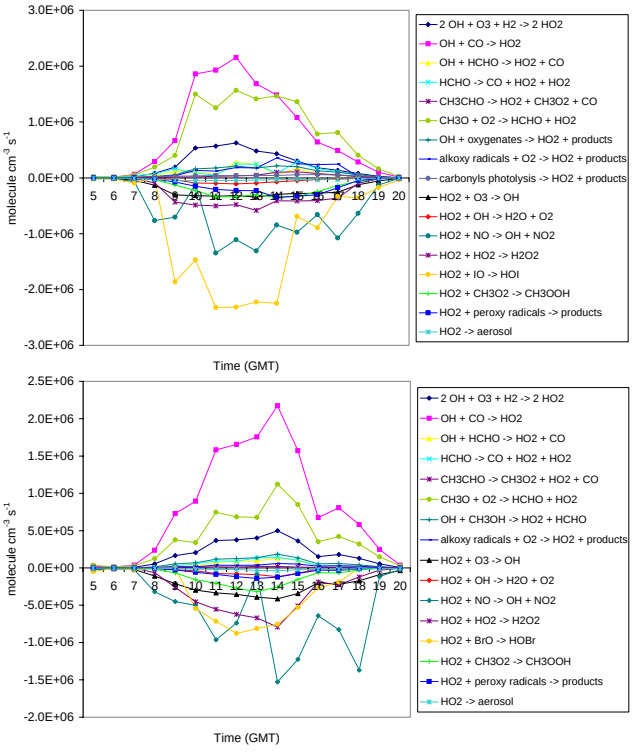

Fig. 10. Rates of production and destruction of HO_2. **(a)** 18 August ("fulloxy-io-het" model), **(b)** 31 August ("fulloxy-bro-het" model). 2 $OH+O_3+H_2 \rightarrow 2\ HO_2$ indicates the sum of the rates of $OH+O_3 \rightarrow HO_2$ and $OH+H_2 \rightarrow HO_2$.

was a source of OH more or less comparable in magnitude to HO_2+O_3 (Fig. 9b). The comparison between 18 and 31 August showed that the impact of HOX photolysis on [OH] was very different if X is iodine or bromine. This reflects the different fates of these intermediates, and the fact that $j(\mathrm{HOBr}) \ll j(\mathrm{HOI})$.

The losses of OH were very similar on both days and they did not show significant differences with respect to the models without halogens and with a simplified heterogenous loss. OH mainly reacted with CO and CH_4, with CO usually about a factor of two more important. On both these days oxygenated compounds played a large role as OH losses. Acetaldehyde, in particular, was one of the main OH losses on 18 August and it became even more important than CO after 14:00 (Fig. 9a). On 31 August, acetaldehyde was the third most important loss of OH (Fig. 9b). The other significant losses of OH were due to hydrogen, ozone, formaldehyde and HO_2 ($1-3\times10^5$ molecule $\mathrm{cm}^{-3}\,\mathrm{s}^{-1}$). Methanol also had an important role, especially on 18 August when its reaction with OH was faster than that with H_2.

Both on 18 and 31 August the main source of HO_2 was the reaction of OH with CO, followed by the reaction of the methoxy radical with O_2. The latter was about 50% and 25% of the former on 18 and 31 August, respectively. These were followed by the reactions with hydrogen and ozone and by the oxidation of formaldehyde and methanol. On 18 August, acetaldehyde photolysis became a source of HO_2 almost as important as H_2 and O_3 in the afternoon (Fig. 10a), due to an increase of about a factor of 4 in $[CH_3CHO]$ in the afternoon. Methanol was an HO_2 source more important than HCHO on 31 August (Fig. 10b).

The reaction with NO was one of the main losses for HO_2 both on 18 August and on 31 August, followed by the self-reaction of HO_2 and the reaction with CH_3O_2, which was comparable to the reaction with O_3 on 18 August, but about 20–30% slower on 31 August. Other peroxy radicals reacting with HO_2 were CH_3CO_3 and the isoprene-derived peroxy radicals. On 18 August HO_2+IO was the primary sink of HO_2 (up to 2.3×10^6 molecule $\mathrm{cm}^{-3}\,\mathrm{s}^{-1}$) for most of the day (Fig. 10a). It was about 40% higher than the reaction with NO, explaining the decrease in the modelled concentration of HO_2 (Fig. 6a). On 31 August the reaction of HO_2 with BrO (Fig. 10b) was more or less comparable with the self-reaction of HO_2 (about 9×10^5 molecule $\mathrm{cm}^{-3}\,\mathrm{s}^{-1}$).

The fact that the impact of BrO was lower than the impact of IO is expected because the rate coefficient of $BrO+HO_2$ was about 4 times lower than the rate coefficient of $IO+HO_2$. It should also be noted that, on both the days

considered here, the uptake rate for HO_2 on aerosol was only $4-5\times10^4$ molecule cm^{-3} s^{-1}. In fact, this analysis referred to the case with low uptake coefficient for HO_2 (0.006 at 298 K). With $\gamma=1$, which is the maximum theoretical value, this process had more influence on [HO_2] and its rate was therefore much higher ($\sim9\times10^5$ molecule cm^{-3} s^{-1}), comparable to the rate of HO_2+NO.

Figures 2 and 3 show that constraining the model to measured oxygenates reduced both [OH] and [HO_2]. This effect arose primarily through the reaction of OH with acetaldehyde (Fig. 9a) and the consequently reduced direct flux from OH to HO_2. This effect was partly offset by the formation of CH_3O_2 from CH_3CO_3 via reaction with NO and RO_2 (and subsequent production of HO_2 via CH_3O_2+NO).

The analysis of the rates of production of OH and destruction of HO_2 and the study of the model-measurement comparisons for OH and HO_2 with and without the halogens highlighted the different behaviour and effect of iodine and bromine oxides. Of course, the only sources of HOI and HOBr were the reactions of IO and BrO with HO_2. Due to the different values of the rate coefficients, the rate of production of HOI was 2.5–3 times the rate of production of HOBr. This comparison must be taken with caution because it refers to two different days, although the levels of HO_2 were similar (Figs. 3b–c).

On 18 August, HOI was mainly photolyzed to OH and I and the uptake of this species on the particles, even with $\gamma=0.6$, was about one third of the rate of photolysis. Since HOBr photolyzes more slowly (j(HOBr) is ~4.5 times lower than j(HOI)), on 31 August the heterogeneous loss was much more significant for this species. The rate of aerosol uptake of HOBr was about 30% higher than the rate of photolysis at midday. This explains the results of the rate of production analysis for OH on 18 August and 31 August shown previously. HOI was a source of OH at least as important as HO_2+NO, while HOBr was comparable to HO_2+O_3. Even more important, due to the strength of the aerosol uptake with respect to photolysis, HOBr effectively removed HO_x radicals from the system while HOI mainly contributed to their cycling.

It is interesting to compare with the results of the analysis of the impact of IO on HO_2 and OH by Bloss et al. (2005). The relative importance of HO_2+IO with respect to the other loss processes of HO_2 and of HOI photolysis with respect to the other sources of OH was calculated for 18–20 August of NAMBLEX using measured concentrations of OH, HO_2, NO_x, O_3 and IO. The heterogeneous uptake of HO_2 was described using a transition regime expression with $\gamma_{HO_2}=0.2$ (Jacob, 2000). Bloss et al. (2005) found that IO accounted for up to 40% of the total loss of HO_2 with 4 ppt of IO (18 August) and that it was usually comparable to or greater than the heterogeneous loss. HOI accounted for about 15% of the total OH production on the same day. In this work, on the same day, the loss of HO_2 due to IO was about 43% of the total loss of HO_2 and the production of OH due to HOI was about 33% at 12:00. These results are very similar to the analysis shown here, but the comparison must be done keeping in mind the differences in the two calculations. First of all, the calculations of Bloss et al. (2005) were performed using only measured data, while in this work the concentrations of OH and HO_2 were calculated by the model. Second, this model used a value for γ_{HO_2} which is more than 30 times lower than that used by Bloss et al. (2005). Also, they took into account only some of the loss processes of HO_2 (i.e. the reactions with IO, NO, O_3, HO_2, CH_3O_2 and aerosol uptake) and in the production of OH (i.e. the reactions of HO_2 with NO and O_3, $O(^1D)$+H_2O and HOI photolysis). While these were the most important reactions involved, they were not the only ones and, as the rate of production and destruction analysis shown here demonstrated, other reactions significantly affected the radical budget. The simpler mechanism and the neglect of OH formation by HO_2+NO in the calculations of Bloss et al. (2005) probably compensated for the lower uptake coefficient of HO_2 used here, so that the two estimates turned out to be very close.

9 Conclusions

The chemistry of OH and HO_2 in the marine boundary layer was studied using a set of zero-dimensional box-models based upon the MCM and constrained to the measurements. Data were taken during the NAMBLEX campaign which took place in Mace Head, Ireland, during the summer of 2002. Calculated OH and HO_2 were compared with the measurements by the FAGE instrument.

The agreement between the model and the measurements was good, in comparison with the combined uncertanties, for OH. On most of the modelled days the model and the measurements were within 25%. The best agreement was on 9–10 August, when the model could also reproduce very well the structure and the daily profile of OH even during sunrise and sunset. In general the agreement with the measurements was better with the "fulloxy" model than with the "clean" and "full" model, highlighting the importance of the oxygenates for the radical budget. The models generally overestimated [HO_2] by about a factor of 2 or more, although they appeared to be able to reproduce the profile of HO_2, in particular during several NO_x events.

By comparison, in two previous model studies at the same location (EASE96 campaign, Carslaw et al., 1999; EASE97 campaign, Carslaw et al., 2002) and using the same modelling approach the model/measurements ratios were 1.4 and 2.4 for OH and 1.1–1.8 and 3.6 for HO_2, respectively.

The base models were modified in order to investigate processes that might be included in the mechanisms to obtain a better agreement with the measurements, in particular with regard to HO_2. Rates of uptake on sea-salt particles were calculated for the relevant species using the extended aerosol dataset taken during NAMBLEX and the transition regime

expression which takes into account both the gas-phase diffusion of the molecule and the mass accommodation process (instead of the free-molecular expression). A simple mechanism extension, which included the reaction of HO_2 with XO and the photolysis and aerosol uptake of HOX was added to the models, which were constrained to the measurements of XO. The objective was to assess the impact of these processes on the modelled concentrations of OH and HO_2.

Modelled [HO_2] decreased by up to 30% as a result of the reaction with IO, while [OH] increased by up to 15% via the photolysis of HOI. The actual impact of iodine chemistry on HO_x, and particularly on OH, was strictly dependent on γ_{HOI}. Decreasing γ_{HOI} by an order of magnitude had a negligible effect on HO_2 (less than 5%) but could increase modelled [OH] by up to 15% (relative to the base model) due to the increased photolysis and reduced loss of HOI on aerosol. When the uptake coefficient of HO_2 was increased to its theoretical maximum (1.0), modelled [HO_2] decreased by up to 40% and OH decreased by about 30%, thus compensating the increase due to the photolysis of HOI.

On the other hand, BrO had the effect of decreasing OH by about 10–20% and HO_2 by about 20–30%, relative to the base model and depending on the approach used for the heterogeneous uptake (γ_{HOBr}=0.6). The higher sensitivity of the model to the treatment of aerosol uptake was due to the lower photolysis rate of HOBr, which was mostly taken up on aerosol, acting as a net radical sink.

The addition of halogen monoxides chemistry to the model had a large impact on the HO_x budget. The reaction of IO was the most important loss of HO_2, up to 60% higher than the reaction with NO, while the reaction with BrO was the third most important loss process of HO_2, roughly comparable to the self-reaction. The photolysis of HOI was the second most important source of OH after ozone photolysis, comparable to HO_2+NO, while HOBr photolysis was less important than the reaction of HO_2 with O_3.

The model studies of the NAMBLEX campaign discussed here demonstrated that both IO and BrO had a significant impact on modelled HO_x. It must be noted, however, that the exact impact of these species depends on several factors for which large uncertainties exist. In particular, the measured uptake rate coefficients of HOI and HOBr determine the extent of the net radical loss due to the halogen oxide chemistry as well as the magnitude of the impact upon OH. While halogen oxide chemistry is necessary to describe the behaviour of HO_2, it cannot completely account for the discrepancies between the model and the measurements, unless IO concentration is an order of magnitude higher than measured by DOAS, assuming homogeneous distribution along the optical path. Saiz-Lopez et al. (2006) have shown that IO was likely to be unevenly distributed and concentrated near the coast at Mace Head. Direct measurements on the distribution of IO are therefore necessary to better understand the role of this species in the HO_x cycle.

In addition, the uptake of HO_2 on sea-salt particles also appears to have a crucial role, and the best agreement is reached when both processes are taken into account. The overall impact of the heterogeneous uptake of HO_2 depends upon the uptake coefficient used, which is very uncertain. Thornton et al. (personal communication) found that γ_{HO_2} depends sensitively on aerosol composition, and in particular on the aerosol phase concentration of oxidizing agents and on pH. Clearly, further characterization and understanding of the processes involved in HO_2 uptake are central to an improved description of HO_2 chemistry in the troposphere.

Acknowledgements. We gratefully acknowledge the support and the help of the Mace Head Atmospheric Research Station during the NAMBLEX campaign, particularly G. Spain. Thanks to G. P. Johnson for technical assistance with the operation of the FAGE instrument during the campaign. We also would like to thank M. E. Jenkin for many useful discussions, J. Methven for providing the back trajectories and the Universities of Leeds, Leicester, East Anglia, Manchester and York for the use of their data. R. Sommariva acknowledges the University of Leeds for a scholarship. D. E. Heard would like to thank the Royal Society for a University Research Fellowship and some equipment funding.

Edited by: A. Hofzumahaus

References

Alicke, B., Hebestreit, K., Stutz, J., and Platt, U.: Iodine oxide in the marine boundary layer, Nature, 397, 572–573, 1999.

Allan, B. J., McFiggans, G., Plane, J. M. C., and Coe, H.: Observations of iodine monoxide in the remote marine boundary layer, J. Geophys. Res., 105, 14 363–14 369, 2000.

Atkinson, R. and Arey, J.: Atmospheric degradation of volatile organic compounds, Chemical Reviews, 103, 4605–4638, 2003.

Bates, T. S., Kapustin, V. N., Quinn, P. K., Covert, D. S., Coffman, D. J., Mari, C., Durkee, P. A., Bruyn, W. J. D., and Saltzman, E. S.: Processes controlling the distribution of aerosol particles in the lower marine boundary layer during the First Aerosol Characterization Experiment (ACE 1), J. Geophys. Res., 103, 16 369–16 383, 1998.

Bates, T. S., Quinn, P. K., Coffman, D. J., Johnson, J. E., Miller, T. L., Covert, D. S., Wiedensohler, A., Leinert, S., Nowak, A., and Neususs, C.: Regional physical and chemical properties of the marine boundary layer aerosol across the Atlantic during Aerosol99: an overview, J. Geophys. Res., 106, 20 767–20 782, 2001.

Bauer, D., Ingham, T., Carl, S. A., Moortgat, G. K., and Crowley, J. N.: Ultraviolet-visible absorption cross sections of gaseous HOI and its photolysis at 355 nm, J. Phys. Chem., 102, 2857–2864, 1998.

Berresheim, H., Elste, T., Tremmel, H. G., Allen, A. G., Hansson, H.-C., Rosman, K., Maso, M. D., Mäkelä, J. M., and Kulmala, M.: Gas-aerosol relationship of H_2SO_4, MSA, and OH: observations in the coastal marine boundary layer at Mace Head, Ireland, J. Geophys. Res., 107, 8100, 2002.

Bloss, W. J., Rowley, D. M., Cox, R. A., and Jones, R. L.: Rate coefficient for the BrO+HO_2 reaction at 298 K, Phys. Chem. Chem. Phys., 4, 3639–3647, 2002.

Bloss, W. J., Lee, J. D., Johnson, G. P., Sommariva, R., Heard, D. E., Saiz-Lopez, A., Plane, J. M. C., McFiggans, G., Coe, H., Flynn, M., Williams, P., Rickard, A. R., and Fleming, Z.: Impact of halogen monoxide chemistry upon boundary layer OH and HO_2 concentrations at a coastal site, Geophys. Res. Lett., 32, L06814, doi:10.1029/2004GL022084, 2005.

Bohn, B., Kraus, A., Muller, M., and Hofzumahaus, A.: Measurement of atmospheric $O_3 \rightarrow O(^1D)$ photolysis frequencies using filter radiometry, J. Geophys. Res., 109, D10S90, doi:10.1029/2003JD004319, 2004.

Brasseur, G. P., Hauglustaine, D. A., Walters, S., Rasch, P. J., Muller, J. F., Granier, C., and Tie, X. X.: MOZART, a global chemical transport model for ozone and related chemical tracers – 1. Model description, J. Geophys. Res., 103, 28 265–28 289, 1998.

Carpenter, L. J.: Iodine in the marine boundary layer, Chem. Rev., 103, 4953–4962, 2003.

Carslaw, N., Creasey, D. J., Heard, D. E., Lewis, A. C., McQuaid, J. B., Pilling, M. J., Monks, P. S., Bandy, B. J., and Penkett, S. A.: Modeling OH, HO_2, and RO_2 radicals in the marine boundary layer – 1. Model construction and comparison with field measurements, J. Geophys. Res., 104, 30 241–30 255, 1999.

Carslaw, N., Bell, N., Lewis, A. C., McQuaid, J. B., and Pilling, M. J.: A detailed case study of isoprene chemistry during the EASE96 Mace Head campaign, Atmos. Environ., 34, 2827–2836, 2000.

Carslaw, N., Creasey, D. J., Heard, D. E., Jacobs, P. J., Lee, J. D., Lewis, A. C., McQuaid, J. B., Pilling, M. J., Bauguitte, S., Penkett, S. A., Monks, P. S., and Salisbury, G.: Eastern Atlantic Spring Experiment 1997 (EASE97) – 2. Comparisons of model concentrations of OH, HO_2, and RO_2 with measurements, J. Geophys. Res., 107, 24 156, 2002.

Chameides, W. L. and Davies, D. D.: Iodine: its possible role in tropospheric photochemistry, J. Geophys. Res., 85, 7383–7398, 1980.

Coe, H., Allan, J. D., Alfarra, M. R., Bower, K. N., Flynn, M. J., McFiggans, G. B., Topping, D. O., Williams, P. I., O'Dowd, C. D., Dall'Osto, M., Beddows, D. C. S., and Harrison, R. M.: Chemical and physical characteristics of aerosol particles at a remote coastal location, Mace Head, Ireland, during NAMBLEX, Atmos. Chem. Phys. Discuss., 5, 11 643–11 678, 2005.

Davis, D., Crawford, J., Liu, S., McKeen, S., Bandy, A., Thornton, D., Rowland, F., and Blake, D.: Potential impact of iodine on tropospheric levels of ozone and other critical oxidants, J. Geophys. Res., 101, 2135–2147, 1996.

DeMore, W. B., Sander, S. P., Golden, D. M., Hampson, R. F., Kurylo, M. J., Howard, C. J., Ravishankara, A. R., Kolb, C. E., and Molina, M. J.: Chemical kinetics and photochemical data for use in stratospheric modeling, Tech. rep., Jet Propulsion Laboratory, Pasadena, California, USA, http://jpldataeval.jpl.nasa.gov/, 2003.

Derwent, R. G., Jenkin, M. E., and Saunders, S. M.: Photochemical ozone creation potentials for a large number of reactive hydrocarbons under European conditions, Atmos. Environ., 30, 181–199, 1996.

Edwards, G. D. and Monks, P. S.: Performance of a single-monochromator diode array spectroradiometer for the determination of actinic flux and atmospheric photolysis frequencies, J. Geophys. Res., 108(D16), 8546, doi:10.1029/2002JD002844, 2003.

Fleming, Z. L., Monks, P. S., Rickard, A. R., Heard, D. E., Bloss, W. J., Seakins, P. W., Still, T. J., Sommariva, R., Pilling, M. J., Morgan, R., Green, T. J., Brough, N., Mills, G. P., Penkett, S. A., Lewis, A. C., Lee, J. D., Saiz-Lopez, A., and Plane, J. M. C.: Peroxy radical chemistry and the control of ozone photochemistry at Mace Head, Ireland during the summer of 2002, Atmos. Chem. Phys. Discuss., 5, 12 313–12 371, 2005.

Gratpanche, F., Ivanov, A., Devolder, P., Gershenzon, Y., and Sawerysyn, J.-P.: Uptake coefficients of OH and HO_2 radicals on material surfaces of atmospheric interest, in: 14th International Symposium on Gas Kinetics, Leeds, 1996.

Haggerstone, A.-L., Carpenter, L. J., Carslaw, N., and McFiggans, G.: Improved model predictions of HO_2 with gas to particle mass transfer rates calculated using aerosol number size distributions, J. Geophys. Res., 110, D04303, doi:10.1029/2004JD005282, 2005.

Heard, D. E. and Pilling, M. J.: Measurement of OH and HO_2 in the troposphere, Chem. Rev., 103, 5163–5198, 2003.

Heard, D. E., Read, K. A., Al-Haider, S., Bloss, W. J., Johnson, G. P., Pilling, M. J., Rickard, A., Seakins, P. W., Smith, S. C., Sommariva, R., Stanton, J. C., Still, T., Brooks, B., Jackson, A. V., McQuaid, J. B., Morgan, R., Smith, M. H., Carpenter, L. J., Carslaw, N., Hamilton, J., Hopkins, J. R., Lee, J. D., Lewis, A. C., Purvis, R. M., Wevill, D. J., Brough, N., Green, T., Mills, G., Penkett, S., Plane, J. M. C., Saiz-Lopez, A., Worton, D., Monks, P. S., Fleming, Z., Alfarra, M., Allan, J. D., Bower, K., Coe, H., Cubison, M., Flynn, M., McFiggans, G., Gallagher, M., Norton, E. G., Shillito, J., Topping, D., Vaughan, G., Williams, P., Bitter, M., Ball, S. M., Jones, R. L., Povey, I. M., ODoherty, S., Noone, C., Simmonds, P. G., Allen, A., Kinnersley, R., Beddows, D., DallOsto, M., Harrison, R. M., Donovan, R., Heal, M., Methven, J., Jennings, G., and Spain, G.: The North Atlantic Marine Boundary Layer Experiment (NAMBLEX). Overview of the campaign held at Mace Head, Ireland in summer 2002, Atmos. Chem. Phys. Discuss., 5, 12 177–12 254, 2005.

Ingham, T., Bauer, D., Landgraf, J., and Crowley, J. N.: Ultraviolet-visible absorption cross sections of gaseous HOBr, J. Phys. Chem., 102, 3293–3298, 1998.

Jacob, D. J.: Heterogeneous chemistry and tropospheric ozone, Atmos. Environ., 34, 2131–2159, 2000.

Jenkin, M. E., Saunders, S. M., and Pilling, M. J.: The tropospheric degradation of volatile organic compounds: a protocol for mechanism development, Atmos. Environ., 31, 81–104, 1997.

Jenkin, M. E., Saunders, S. M., Wagner, V., and Pilling, M. J.: Protocol for the development of the Master Chemical Mechanism, MCMv3 (Part B): tropospheric degradation of aromatic volatile organic compounds, Atmos. Chem. Phys., 3, 181–193, 2003.

Jennings, S. G., Kleefeld, C., O'Dowd, C., Jinker, C., Spain, T. G., O'Brien, P., Roddy, A. F., and O'Connor, T. C.: Mace Head Atmospheric Research Station – Characterization of aerosol radiative parameters, Boreal Environ. Res., 8, 303–314, 2003.

Kanaya, Y., Sadanaga, Y., Matsumoto, J., Sharma, U. K., Hirokawa, J., Kajii, Y., and Akimoto, H.: Daytime HO_2 concentrations at Oki Island, Japan, in summer 1998: comparison between

measurement and theory, J. Geophys. Res., 105, 24 205–24 222, 2000.

Kanaya, Y., Matsumoto, J., Kato, S., and Akimoto, H.: Behavior of OH and HO_2 radicals during the observations at a remote island of Okinawa (ORION99) field campaign – 2. Comparison between observations and calculations, J. Geophys. Res., 106, 24 209–24 223, 2001.

Kanaya, Y., Yokouchi, Y., Matsumoto, J., Nakamura, K., Kato, S., Tanimoto, H., Furutani, H., Toyota, K., and Akimoto, H.: Implications of iodine chemistry for daytime HO_2 levels at Rishiri Island, Geophys. Res. Lett., 29, 1212, 2002.

Knight, G. P. and Crowley, J. N.: The reactions of IO with HO_2, NO and CH_3SCH_3: flow tube studies of kinetics and product formation, Phys. Chem. Chem. Phys., 3, 393–401, 2001.

Kraus, A. and Hofzumahaus, A.: Field measurements of atmospheric photolysis frequencies for O_3, NO_2, HCHO, CH_3CHO, H_2O_2, and HONO by UV spectroradiometry, J. Atmos. Chem., 31, 161–180, 1998.

Lewis, A. C., Hopkins, J. R., Carpenter, L. J., Stanton, J., Read, K. A., and Pilling, M. J.: Sources and sinks of acetone, methanol, and acetaldehyde in North Atlantic air, Atmos. Chem. Phys., 5, 1963–1974, 2005.

McFiggans, G., Plane, J. M. C., Allan, B. J., Carpenter, L. J., Coe, H., and O'Dowd, C.: A modeling study of iodine chemistry in the marine boundary layer, J. Geophys. Res., 105, 14 371–14 385, 2000.

Methven, J., Evans, M., Simmonds, P., and Spain, G.: Estimating relationships between air mass origin and chemical composition, J. Geophys. Res., 106, 5005–5019, 2001.

Monks, P. S., Rickard, A. R., Hall, S. L., and Richards, N. A. D.: Attenuation of spectral actinic flux and photolysis frequencies at the surface through homogeneous cloud fields, J. Geophys. Res., 2004.

Morgan, R. B. and Jackson, A. V.: Measurements of gas-phase hydrogen peroxide and methyl hydroperoxide in the coastal environment during the PARFORCE project, J. Geophys. Res., 107, 8109, 2002.

Mössinger, J. C. and Cox, R. A.: Heterogeneous reaction of HOI with sodium halide salts, J. Phys. Chem., 105, 5165–5177, 2001.

Norton, E. G., Vaughan, G., Methven, J., Coe, H., Brooks, B., Gallagher, M., and Longley, I.: Boundary layer structure and decoupling from synoptic scale flow during NAMBLEX, Atmos. Chem. Phys., 6, 433–445, 2006.

Olson, J. R., Crawford, J. H., Chen, G., Fried, A., Evans, M. J., Jordan, C. E., Sandholm, S. T., Davis, D. D., Anderson, B. E., Avery, M. A., Barrick, J. D., Blake, D. R., Brune, W. H., Eisele, F. L., Flocke, F., Harder, H., Jacob, D. J., Kondo, Y., Lefer, B. L., Martinez, M., Mauldin, R. L., Sachse, G. W., Shetter, R. E., Singh, H. B., Talbot, R. W., and Tan, D.: Testing fast photochemical theory during TRACE-P based on measurements of OH, HO_2 and CH_2O, J. Geophys. Res., 109, D15S10, doi:10.1029/2003JD004278, 2004.

Saiz-Lopez, A. and Plane, J. M. C.: Novel iodine chemistry in the marine boundary layer, Geophys. Res. Lett., 31, L04112, doi:10.1029/2003GL019215, 2004.

Saiz-Lopez, A., Plane, J. M. C., and Shillito, J. A.: Bromine oxide in the mid-latitude marine boundary layer, Geophys. Res. Lett., 31, L03111, doi:10.1029/2003GL018956, 2004.

Saiz-Lopez, A., Shillito, J. A., Coe, H., and Plane, J. M. C.: Measurements and modelling of I_2, IO, OIO, BrO and NO_3 in the mid-latitude marine boundary layer, Atmos. Chem. Phys. Discuss., 5, 9731–9767, 2005.

Saiz-Lopez, A., Plane, J. M. C., McFiggans, G., Williams, P. I., Ball, S. M., Bitter, M., Jones, R. L., Hongwei, C., and Hoffmann, T.: Modelling molecular iodine emissions in a coastal marine environment: the link to new particle formation, Atmos. Chem. Phys., 6, 883–895, 2006.

Sander, R.: Modeling atmospheric chemistry: interactions between gas-phase species and liquid cloud/aerosol particles, Surveys in Geophysics, 20, 1–31, 1999.

Saunders, S. M., Jenkin, M. E., Derwent, R. G., and Pilling, M. J.: Protocol for the development of the Master Chemical Mechanism, MCMv3 (Part A): tropospheric degradation of non-aromatic volatile organic compounds, Atmos. Chem. Phys., 3, 161–180, 2003.

Smith, S. C., Lee, J. D., Bloss, W. J., Johnson, G. P., and Heard, D. E.: Concentrations of OH and HO_2 radicals during NAMBLEX: measurements and steady-state analysis, Atmos. Chem. Phys. Discuss., 5, 12 403–12 464, 2005.

Sommariva, R., Haggerstone, A.-L., Carpenter, L. J., Carslaw, N., Creasey, D. J., Heard, D. E., Lee, J. D., Lewis, A. C., Pilling, M. J., and Zádor, J.: OH and HO_2 chemistry in clean marine air during SOAPEX-2, Atmos. Chem. Phys., 4, 839–856, 2004.

Still, T. J., Al-Haider, S., Seakins, P. W., Sommariva, R., Stanton, J. C., Mills, G., and Penkett, S. A.: Ambient formaldehyde measurements made at a remote marine boundary layer site during the NAMBLEX campaign – a comparison of data from chromatographic and modified Hantzsch techniques, Atmos. Chem. Phys. Discuss., 5, 12 531–12 567, 2005.

Tan, D., Faloona, I., Simpas, J. B., Brune, W., Olson, J., Crawford, J., Avery, M., Sachse, G., Vay, S., Sandholm, S., Guan, H. W., Vaughn, T., Mastromarino, J., Heikes, B., Snow, J., Podolske, J., and Singh, H.: OH and HO_2 in the tropical Pacific: results from PEM Tropics B, J. Geophys. Res., 106, 32 667–32 681, 2001.

Wachsmuth, M., Gaggeler, H. W., von Glasow, R., and Ammann, M.: Accommodation coefficient of HOBr on deliquescent sodium bromide aerosol particles, Atmos. Chem. Phys., 2, 121–131, 2002.